Comparative Analysis of Hydrocarbon Generation by Probable Source Rocks in the Deep and Uplifted Parts of the East Barents Basin: Results from Basin Modeling*

Yurii Galushkin[1], G. E. Yakovlev[1], and K. A. Sitar[1]

Search and Discovery Article #10566 (2014)
Posted January 27, 2014

*Adapted from an extended abstract given as a poster presentation at AAPG 3P Arctic Polar Petroleum Potential Conference & Exhibition, Stavanger, Norway, October 15-18, 2013

[1]Lomonosow Moscow State University, Leninskie Gory, Russia (yu_gal@mail.ru, sitar_msu@mail.ru)

Abstract

For assessment of oil-gas perspective of the East Barents region, we compared the thermal and HC generation histories of the Paleozoic, Mesozoic and Cenozoic sedimentary rocks in the South Barents depression with the histories of the Admiralteyskoe rise. Our analysis is based on numerical modeling in the frame of the GALO basin modeling system, which was carried out for Krestovaya, Admiralteyskaya and Pachtusova areas in the Admiralteyskoe rise, for Ludlovskaya, Ledovaya, Shtokmanovskaya, Arkticheskaya areas in the South Barents depression.

Evolution of the lithosphere in the South Barents depression includes the continental rifting in the Devonian and considerable thinning of the crust in the Permian and Triassic ($\beta \approx 2$), associated with intensive sedimentation. Radioactive heat of thick sedimentary cover contributes sufficiently in recent heat flow of the region. The modeling suggests more intensive thermal activation of the lithosphere in the northern areas that in the southern ones. It corresponds to increase in present-day heat flow toward the North.

According to the modeling, liquid hydrocarbons generated by the Ordovician, Silurian and Devonian deposits in the Admiralteyskaya and Pachtusova areas and by Devonian, Permian and considerable part of Triassic rocks in the South Barents depression were subjected (perhaps, partly) to secondary creaking. The Carboniferous, Permian and Lower Triassic rocks at the depths of 1,000 - 3,600 m in the present-day section of Admiralteyskaya and Pachtusova areas are predominantly oil generating, whereas deeper horizons can be considered as gas prone. In the recent sections of the Ledovaya, Shtokmanovskaya and Arkticheskaya areas, the rocks at the depths of 2,500 - 4,200 m are oil prone.

Thus, sufficient part of the Permian-Triassic deposits in center of the South Barents depression occurs within the gas generation zone. Migration of gas hydrocarbons toward the East can be reason of movement of oil accumulations to the same direction. Formation of secondary oil and gas deposits can be caused also due to step-rising migration of hydrocarbons along the tectonic dislocations in the eastern slope of the Admiralteyskoe rise.

Introduction

A number of gas and gas-condensate deposits were discovered in the East-Barents Basin: the Murmanskoye, Severo-Kaldinskoye and Luninskoye gas fields, the Stokman, Ludlov and Ledovoye gas-condensate fields (Figure 1; Bogdanov and Khain, 1996). These giant gas and gas-condensate fields locate in the East Barents depression and are assumed to form due to thermal creaking of organic matter in the Early-Mesozoic and Paleozoic sediments and only in small extent by creaking of Jurassic organic matter (OM). In recent time the uplifted areas of the East Barents Basin like to the Admiralteyskoe and Fedynskoe rises are considered also as perspective areas for oil and gas exploration. In our paper an attempt is made to compare numerically a hydrocarbon generation by probable source rocks in the deep and uplifted areas of the East Barents sedimentary Basin. The reconstructions for Krestovaya, Admiralteyskaya and Pachtusova areas in the Admiralteyskoe Rise and for Ludlovskaya, Ledovaya, Shtokmanovskaya, Arkticheskaya areas in the South Barents depression are carried out and two sedimentary sections near the Arctic and Admiralteyskaya wells are considered in detail (Figure1).

Comparison is based on refined structure and composition of the sedimentary sections and new measured values of deep temperature and vitrinite reflectance. Numerical reconstructions of the burial, thermal and maturation histories of the Basin were carried out with application of the GALO system of basin modeling (Makhous et al., 1997, Makhous and Galushkin, 2003, 2005; Galushkin et al., 2014).

Geological and Geophysical Description of the Region

Two deep sedimentary depressions with the depth of the basement surface of 16-18 km up to 20-23 km were discovered seismically in the eastern part of the Barents shelf: the South- and North-Barents basins (Figure 1; Shipilov and Mossur, 1990; Bogdanov and Khain, 1996; Kogan and Mursin, 1997; Applonov, 2000). The South Barents basin is separated from the North Barents by the Ludlov saddle with depth of the basement at about of 12 km. The trough of the Barents sea paleorift formed in the Middle-Late Devonian across both of the basins from the north to the south at distance about 1,500 km. The width of the rift area ranges from 300 to 600 km. In the axial part of the rift, a considerable thinning of the granite layer (up to total declining) is assumed. The Moho boundary rises here up to depth of 28-32 km in the South Barents depression and to 32-34 km in the North Barents depression. It is equal to 42-45 km in the western, eastern and southern margins of the depressions (Neprochnov et al., 2000; Kogan et al., 2002). The crust stretching resulted in thinning of granite layer by 10 km compared with the basin flank areas (Figure 2; Neprochnov et al., 2000).

The thickness of sedimentary cover in the South and North Barents depressions reached 20-23 km, decreasing to 5-7 km at the flanks of the depressions (Kogan et al., 2002). The basin evolution began with continental rifting in the Middle Devonian and finished by long erosion in the Upper Cretaceous – Cenozoic (Figure 3). Fast subsidence of the basins in the Late Permian – Early Triassic resulted from intensive extension of the basin lithosphere in Permian-Triassic (Gramberg, 1997; Korotaev et al., 1998; Gramberg et al., 2001). The sedimentation in the Permian-Triassic was intensive in the rest of the Barents-Karskaya plate, but with lesser thicknesses of depositions (Gramberg, 1997). Composition of the Permian-Triassic depositions is terrigenous and changes phacially from lacustrine-continental at the south to shallow marine at the north.

Numerical simulation of burial and thermal histories of sedimentary section in the East Barents shelf

The GALO Basin Modeling System

Numerical reconstructions of the basin evolution considered in our paper were carried out using the GALO program package for basin modeling. Similar to another basin modeling systems (Ungerer et al., 1990; Welte et al., 1997), the GALO uses geological and geophysical data based on structure and evolution of the basin in order to reconstruct numerically the burial history of the sedimentary basin, calculate the rock temperature variations and degree of organic matter maturation and estimate realization of hydrocarbon potential of the basin (Makhous and Galushkin, 2005). In addition to traditional tasks of basin modeling, GALO solves some specific problems of basin modeling, which can not be analyzed in the frame of traditional geothermic approaches, such as an assessment of amplitude of the thermal and tectonic reactivation of the basin lithosphere from tectonic subsidence analysis, formation of temperature and maturation distribution with depth as result from hydrothermal-intrusive activity (Galushkin, 1997a, b; Makhous and Galushkin, 2005; Galushkin et al., 2013: 2014).

Burial History of the basin

Figure 3 and Figure 4 demonstrate an evolution of the depth of sedimentary layers during burial history of the East Barents Sea basin on the Pachtusov, Admiralteyskaya, Krestovaya, Lydlov, Ledovaya, Shtockman and Arctic areas. The consolidation of sediments is considered in the GALO system in the usual approach, when a change in matrix volume due to compression is considered as negligible in comparison with the deformation of porous media. (Perrier and Qublier, 1974). We suggest that porosity decreases with depth exponentially. Parameters of rock consolidation in this exponential dependence depended on rock lithology. The rocks of sedimentary sections in the studied region are presented by different fractions of clays, shales, aleurolite, sandstones, and limestones. According to seismic data, thickness of sedimentary cover in the Ledovaya, Shtockman and Arctic areas exceeds 15 km; it is more than 12 km at the Ludlov area and ranges from five to nine kilometers at the areas of the Admiralteyskoe rise (Figure 3 and Figure 4).

All of the areas analyzed here are characterized by maximal sedimentation rates in the Lower Triassic. These rates increase toward the southern part of the East Barents Basin. As whole, the sedimentation rates diminish considerable in the Jurassic, Cretaceous and Cenozoic up to considerable erosion in the areas within the Admiralteyskoe Rise (Figure 3). As result of such burial history, the Devonian and Carboniferous deposits occur at depths of 3,600 m $\leq z \leq$ 5,000 m in the present section of the Admiralteyskaya and Pachtusova areas and subsided to depths more than 12 km in the Ledovaya, Shtockman and Arctic areas.

Thermal History of the Basin

Temperature distribution within the sedimentary cover and underlying lithosphere was found out from numerical solution of heat-transfer equation, scribed in the frame related with the basement. Temperature at the upper boundary of the computation domain (Z=0) changes with geological time according to paleoclimate conditions of the basin development (upper Figure 3a and Figure 4a). For the Carboniferous – Late Cretaceous the paleoclimate curves was given from the papers (Frakes, 1979; Welte et al., 1997) and for the Cenozoic – from (Velichko, 1987; 1999). The steady temperature Tlow ≈ 1,150° - 1,160ºC was maintained at the base of the domain (Z≈100 – 120 km). Initial temperature

distribution corresponded to the values of surface temperature and heat flow during initiation period of the basin evolution. The value of initial heat flow was corrected in accordance with variations in tectonic subsidence of the basement surface (Galushkin and Yakovlev, 2004; Makhous and Galushkin, 2005). Non-steady heat transfer equation was solved using the non-apparent finite-difference scheme adapted for variable thermal physical parameters in the equation and for non-steady time and depth steps. The depth steps (Δz) change continually from 1 - 2 m near surface of the basin to 10-30 m at its base of sedimentary cover. Within the basement, Δz increase linearly up to 2,000-3,000 m at the base of the computed domain ($Z \approx 100 - 120$ km). A validity of the difference scheme was verified by comparison numerical results with analytical (Carslaw and Yaeger, 1959; Turcotte and Schubert, 1982) and semianalytical (Golmshtock, 1979, 1980; Galushkin and Smirnov, 1987) solutions for deposition of homogenous uncompressed sediments with steady rate on homogenous basement, and by comparison between solutions received by using of different steps Δt and Δz (Makhous and Galushkin, 2005).

The values of thermal physical parameters in the heat transfer equation are determined by lithological rock composition, rock porosity and temperature. These values change considerable with time of the basin evolution and depth. For example, heat conductivity of argillaceous sandstone increases from 1.2 – 1.3 W/mºK at small depths to 3 – 3.5 W/mºK at the depth of more than 4-5 km. Such variations in heat conductivity resulted in significant variations in thermal gradient at all of the stages of the basin development including the modern one (Figure 3, Figure 4, Figure 5, Figure 6). At whole, heat conductivities computed in our model were in well agreement with the values measured for the region rocks presented in the paper (Tsybulay and Levashkevich, 1992).

The contribution of radiogenic heat generation from sedimentary rocks is the main reason of difference in heat flows through the surface of sediments and the basement in Figure 8. This contribution into surface heat flow reaches to 20-25 mW/m^2 for thick sedimentary covers in the Ledovaya, Shtockman, and Arctic areas and to about eight mW/m^2 for thinner covers of the Admiralteyskaya and Packtusov areas.

Heat Flow and Thermal State of the Basin

In the modeling, we suggested that the basement of the East Barents Sea Basin before its extension in the Devonian and Permian-Triassic was presented by standard continental lithosphere that includes granite layer of thickness of 15 km with higher radiogenic generation in the upper 5 km (Bayer, 1981) and pseudo-basalt layer of the thickness of 20 km. As whole, radiogenic contribution of the initial lithosphere (before its extension in the Devonian and Permian-Triassic) into surface heat flow was about 25 mW/m^2. According to the modeling, amplitude of the lithosphere extension in the Ledovaya, Shtockman and Arctic areas, located near to paleorift axis (Figure 1), reached to 2.0 – 2.1, whereas in the Admiralteyskoe Rise it consisted only $\beta \approx 1.15$ in the Devonian and $\beta \approx 1.20$ in the Permian-Triassic. Then, the present-day heat flow from the mantle can be assessed roughly by reducing the radiogenic contribution of thinned crust (about 12 mW/m^2 for the Ledovaya, Shtockman and Arctic areas and 19 mW/m^2 for Admiralteyskaya area) from the calculated heat flow through the basement surface (31 – 34 mW/m^2 for the first three areas and 63 mW/m^2 – for the Admiralteyskaya area). Therefore, modern mantle heat flow is about 19 – 22 mW/m^2 in the Ledovaya, Shtockman and Arctic areas, but increase considerable to the north, reaching in the Admiralteyskaya area about 44 mW/m^2 . This increase of mantle heat flow can be related with approach to modern spreading centre – the Gakkel ridge, located to the north from the region under study.

In this connection, it is necessary to say a few words about the discrepancy calculated and measured values of surface heat flow. One of the problems in modeling of thermal regime of the East Barents Basin is a considerable contradiction between high values of heat flow measured in

the region and relatively low values of deep temperatures and degree of organic matter maturation, measured in wells. Indeed, measured heat flow is about 70 mW/m^2 in the Ledovaya, Shtockman and Arctic areas and about 90 mW/m^2 in the Admiralteyskaya area (Verzhbitsky, 2000, 2002; Khutorskoy and Podgorny, 2001). These values exceed the ones calculated in our model which consist 53.4, 56.2, 58.1 mW/m^2 in the Ledovaya, Shtockman and Arctic areas and 71 mW/m^2 in the Admiralteyskaya area. The corrections on the Quaternary climate variations could only decrease calculated flows. On the other hand, the deep temperatures calculated in the model are in reasonable agreement with the reliable measured ones (see Figure 5 and Figure 7 for the Admiralteyskaya and Arctic areas). So, in the Arctic area at the depth z = 2,600 and 4,050 m, calculated temperatures T = 88°C and 119°C, whereas measured values T = 90 and 122°C, correspondingly (Figure 7). In the same time, we must obtain more high temperatures T = 115°C and 159°C at the same depths if we taken in the Arctic area measured surface heat flow equaled to 69 mW/m^2 (in this case the heat flow through the basement surface would be 48.5 mW/m^2). Similar situation takes place with vitrinite reflectance. Here we become Ro = 2.02% at depth z=4,050 m for heat flow q=69 mW/m^2 whereas measured value is Ro=0.90% (see below). Calculations show that application of measured heat flow q = 70 mW/m^2 to modeling of the Ledovaya, Shtockman and Arctic areas led to overestimation of temperatures by 30-40°C and considerable overstating in the %Ro values. Corrections on the Quaternary climate variations must only enhance the above contradiction. Khutorskoy and Podgorny (1998; 2001) who faced a similar problem in his model of the thermal state of the lithosphere of the East Barents Basin, believe that the above contradiction is related to the hardness of heat flow measurements in the shelf, because numerous distortions of heat flow by exogenic and near surface factors led to considerable scatter in the measured values of heat flow. They concluded that the reliable method of heat flow measurement is only its measurement in deep wells. We note in passing that measured heat conductivities of aleurolite and sandstone samples from depth of 1,440 and 3,100 m in the Shtockman area are in agreement at accuracy 10-20% with the values computed in our basin model. The measurements of deep temperatures in the well with enough time after drilling stops (the Arctic and Admiralteyskaya wells; Tsybulya and Levashkevich, 1992) are more reliable for modeling control than heat flow measurements. That is why we used the deep temperature measurements but no heat flow measurements to control the modeling results.

An evolution of the thermal regime of the lithosphere in the East Barents region is shown in Figure 8 on the example of the Arctic and Admiralteyskaya areas. This evolution includes the Devonian continental rifting and considerable crust thinning in the Permian-Triassic. As a result from intensive crust thinning ($\beta \approx 2$ in southern areas of the Basin; see next section), the MOHO boundary moved upward in this time, despite the fact that sedimentation was very quick (Figure 4 and Figure 8). The Permian crust thinning was accompanied by significant heating of the basin lithosphere (upper Figure 8). The modeling assumes a more intensive thermal activation of the basin lithosphere in the Cenozoic in the northern areas than in the southern (Figure 8). This is in accordance with increase of heat flow to the North with approach to the Gakkel Ridge. In addition, we note that the lithosphere in the Ledovaya, Shtockman and Arctic areas is characterized by more high heat flow than the one in the southern areas (such as Pomorian and Prirazlomnaya).

The study region is characterized by rather high thermal regime. So the temperatures of the rocks at the base of sedimentary sections in the Arctic, Shtockman and Ledovaya areas at the depth of 16,500, 16,000, and 17,700 m reach 340, 363 and 386°C, respectively (Figure 4; Table 2). They reach 160°C at the depth about of six kilometers in the Admiralteyskaya area (Figure 3; Table 1). As whole, thermal evolution of sedimentary cover is in agreement with the thermal variations of the lithosphere (Figure 8), but they were complicated by climate variations and sedimentation rates (Figure 3 and Figure 4).

An Analysis of Tectonic Subsidence of the Basin

In addition to temperature and maturation (see below), an analysis of the Basin's tectonic subsidence is used also as one of control factors of the modeling (Figure 9). This analysis suggested an isostatic response of the lithosphere on the load. Isostasy level was accepted at the base of the domain for calculation (Z≈120-150 km). Therefore, it was located within the deep, heated horizons of the mantle, the rocks of which are rheologically weak and able to flow under small strength difference. Deviations from isostasy should not be great as at the stages of weakening of the lithosphere during its heating or extension, as in normal stage when the typical horizontal size of sedimentary cover exceeds considerably the effective elastic thickness of the lithosphere.

An analysis of tectonic subsidence of the basement is used in our modeling to estimate the sequence and amplitude of tectonic-thermal events, which could occur during the basin evolution (Galushkin and Yakovlev, 2004: Makhous and Galushkin, 2005; Galushkin et al., 2014). The variations in the basement tectonic subsidence are computed by two independent methods. The first calculates the response of the lithosphere caused by removing of water and sediments load. These variations in the basement tectonic subsidence are shown in Figure 9 by solid lines. In the second method, tectonic subsidence is determined from the time-variations in density distribution with depth within the basement. The weight of the basement column is calculated at every time step of modeling. In these calculations, density of the lithosphere rocks ρl (Z,t) is a function of temperature T(Z,t) and pressure P(Z,t):

$$\rho_l(Z,t) = \rho_0(Z,t)\cdot[1-\alpha\cdot T(Z,t)+\beta\cdot P(Z,t)]$$

where α is the thermal expansion coefficient, β is the isothermal compressibility of the rock, ρ_o(Z,t) is the density at the standard conditions P=1 atm and T=20°C. The parameter ρo reflects variation in the rock type versus depth (crust, mantle, "granitic" or "basaltic" rock, the compositional transition in the mantle (Forsyth and Press, 1971), and the possible changes in the density distribution within the basement due to basement stretching. The corresponding variations in the basement tectonic subsidence are shown in Figure 9 by dashed lines. Both of the tectonic curves (solid and dashed) must coincide at local isostasy response of the basin lithosphere on internal and external load. The assumed thermal reactivation or extension of the lithosphere changes density distribution in the basement. An amplitude and duration of the event are chosen to ensure coinciding the dashed tectonic line with the solid, provided that the chosen parameters do not contradict to available geological and geophysical information about structure and evolution of the region (Figure 9; Galushkin and Yakovlev, 2004; Makhous and Galushkin, 2005; Galushkin et al., 2014). A special modification of the GALO system is applied to correct the thermal history of the basins with taking into consideration the climate variations in the Pliocene-Holocene when permafrost could arise or degrade (Galushkin, 1997a).

Tectonic analysis allows an assessment of intensity and duration thermal activations of the basin, extension amplitude in the Permian-Triassic and intensity Cenozoic thermal activation, accompanied by the basin erosion. (Figure 3, Figure 4, Figure 9). The modeling suggests a thinning of the basin crust with amplitude β = 2 – 2.15 for the Ledovaya, Shtockman and Arctic areas and β = 1.25 – 1.35 for the areas of the Admiralteyskoe rise. It is interesting that about 30% of the total crust thinning in the Ledovaya area was in the Devonian and 70% - in the Permian-Triassic. According to the analysis, the crust extension in the Arctic and Shtockman areas took place only in the Permian-Triassic, whereas in the Admiralteyskoe rise it was in the Devonian with amplitude of 1.15 and in the Middle and Upper Triassic with amplitude about

of 1.20. The later extension coincides with the period of most intensive subsidence of the basin (Figure 3, Figure 4, Figure 8, and Figure 9). However, we must remember that the above conclusions are based in considerable extent on the accepted chronology of the sedimentary layers, which is rather approximately for the deep horizons of the Permian, Carboniferous and Devonian.

Evolution of maturation degree of organic matter during burial history of the East Barents Sea Basin

Reconstructions of thermal history of sedimentary rocks are used to calculate numerically the variations in catagenesis transformation of organic matter. We estimated the level of the organic matter catagenesis due to calculation a vitrinite reflectance Ro (%) by using of the kinetic spectrum of vitrinite maturation from (Sweeney, Burnham, 1990). Makhous and Galushkin (2005) discuss the algorithm of calculation in detail. Dotted lines in Figure 5, Figure 6, Figure 7, and Figure 8 represent the depths of the Ro-isolines during burial history of the basin. Quick subsidence of the basin in the Permian-Triassic resulted in significant increase of rock temperatures and early maturation of organic matter in the Devonian and Triassic formations in the Ludlov, Ledovaya, Shtockman and Arctic areas (Figure 3 and Figure 4). Even the Low Jurassic rocks at these areas are characterized by rather high catagenesis (Ro ≈ 0.70 – 0.80%; Figure 3 and Figure 4; Table 1, Table 2). The rocks of the same age in the Admiralteyskaya area are less mature due to lesser subsidence (Figure 3; Table 1). Unfortunately, comparison between measured and computed values of Ro can be carried out only for upper horizons of sedimentary sections (Figure 10, Figure 11, and Figure 12). In the Admiralteyskaya and Pakhtusov areas, there are no measurements of vitrinite reflectance, but high thermal regime suggests rather quick increase catagenesis level with depth, that is confirmed partly by data from the Krestovaya area (Figure 10).

In addition to heat flow problems discussed above, there are some problems with assessments of vitrinite reflectance in the Barents Sea region. Our estimation of Ro in the Ledovaya, Shtockman and Arctic areas in Figure 10, Figure 11, and Figure 12 differ from the values predicted for depth more than 4 km by Gramberg et al. (2001) (see Table 1 in cited paper). So, “oil windows” (0.70% ≤ Ro ≤, 1.30%) are located at depths from 2,700 to 4,200 m in our model (Figure 3, Figure 4, Figure 10, Figure 11, and Figure 12), whereas it occupies the depth interval from 3,000 to 6,500 m in the paper by Gramberg et al., (2001). Level of maturity with Ro=2.00% is reached at depth of 5,500 m in our model and at the depth of 10,000 – 11,000 m in the paper cited above. It is necessary to note that the method of statistical interpolation of the Ro-values measured at upper 2-3 km of sedimentary cover to more deep horizons applying in Gramberg et al. (2001) cannot be applied to distribution of Ro with depth in the study region. Calculations of Ro-distributions versus depth carried out with correct kinetic model of vitrinite maturation (Figure 3, Figure 4, Figure 10, Figure 11, and Figure 12), show that the approach of the cited paper must underestimate considerably maturation level at such depth even if gradient of Ro instead the Ro-values will be used in interpolation procedure. Low maturation level of OM, when the “oil window” continues up to depth of 6-7 km, contradicts obvious predominance of gaseous HC over oil in the hydrocarbon accumulations of the region. This fact is in agreement with results of our modeling and suggests more high level of organic matter maturation at the deep horizons of the basin.

Modeling of realization history of hydrocarbon potential for sedimentary rocks of the East Barents Sea shelf

Calculations of HC generation during burial history of formations in the East Barents Sea basin were carried out based on reconstructions of thermal history of the basin discussed above and kinetic spectrum of primary and secondary creaking. Algorithm of calculations is described in Makhous and Galushkin (2005). Secondary creaking of liquid HC can result in total destruction of oil similar to situation in the formations of

the Middle Devonian in all of the considered areas of the basin (Figure 13 and Figure 14) or only partial transformation of liquid HC into gaseous fraction as it took place in the Upper Devonian and Carboniferous formations in the Pakhtusov and Admiralteyskaya areas (Table 1). In our computations, we use kinetic parameters for reactions of primary and secondary creaking of standard kerogenes of types I, II and III, published in the papers of the Paris Oil Institute and the Lavmore Laboratory (Tissot et al., 1987; Espitalie et al., 1988; Burnham, Sweeney, 1989; Burnham and Braun, 1990; Ungerer, 1993 and others).

In our computations, organic matter (OM) in the Ordovician, Silurian and Lower Devonian rocks, and also rocks of the Famenian formation and Carboniferous in the Admiralteyskaya and Pakhtusov areas were presented by the kerogene of type II with initial potential of hydrocarbon (HC) generation Hio= 377 mg HC/g Corg with initial Corg = 0.3 – 0.4%. However, in the southern areas, including the Krestovaya one, Corg in the Carboniferous formations reached 1% and OM were presented by the mixture of 30% kerogene of type I with Hio= 911 mg HC/g Corg, 50% kerogene of type II with Hio=627 mg HC/g Corg, and 20% kerogene of type III with Hio=160 mg HC/g Corg. It corresponds to summary initial hydrocarbon potential Hio=619 mg HC/g Corg. OM of the rocks of the Givetian and Eifelian stages of the Middle Devonian in the Admiralteyskaya and Pakhtusov areas and also the Permian OM in all of the areas of the basin were presented by the mixture of 50% kerogene of type II with initial potential of HC generation Hio= 377 mg HC/g Corg and 50% kerogene of type III with Hio=160 mg HC/g Corg, that corresponds to summary initial hydrocarbon potential Hio=268 mg HC/g Corg.

The present day organic matter content in these formations was about Corg = 0.4%. The Givetian and Eifelian rocks in the southern areas of the basin including the Krestovaya area are characterized by more high value of Corg = 0.6% and were presented by the mixture of 70% kerogene of type II with initial potential of HC generation Hio= 627 mg HC/g Corg and 30% kerogene of type III with Hio=160 mg HC/g Corg, that corresponds to summary initial hydrocarbon potential Hio=487 mg HC/g Corg (Table 1). The Frasnian rocks of the Upper Devonian are characterized by high Corg = 2.0% and are presented by the mixture of 50% kerogene of type I with initial potential of HC generation Hio= 710 mg HC/g Corg and 50% kerogene of type II with Hio=627 mg HC/g Corg, that corresponds to summary initial hydrocarbon potential Hio=688.5 mg HC/g Corg.

Thus, the present day OM content is very low (Copr=0.3 – 0.4%) excluding the Frasnian rocks and the rocks of the Upper Carboniferous in southern areas of the basin. The values of Corg take a part in assessment the start times of primary migration of liquid HC from source rocks (texp in Table 1 and Table 2). These times are noted by vertical lines in Figure 13 and Figure 14 and presented in Table 1 and Table 2. It is known that reaching of expulsion threshold is dependent on many factors: type of OM, content of gaseous phase in generated oil, pressure, temperature of the HC fraction and others (Tissot et al., 1987; Espitalie et al., 1988). The time of initiation of primary migration of liquid HC was determined in our model from condition that liquid HC's fill 20% of porous volume in source rocks or (when the above threshold was not reached) from the condition that the generation of liquid HC reaches 150 mg HC/g Corg. The expulsion threshold determined by such criteria was reached in deep Ordovician, Devonian, Permian and Triassic formations, in spite of low values of Corg in the present day section. It occurred as due to high level of realization of HC potential (Table 1 and Table 2; Figure 13 and Figure 14), as due to decrease in porous volume with depth. Some role here can play the fact that initial Corg can exceed by two and more times the present day Corg, that took into consideration in our procedure of threshold assessment. Therefore, in the Ordovician and Silurian rocks initial Corg was about 0.96%, whereas its present day value is 0.4%. Similar relationships for other formations can be seen in Table 1 and Table 2.

Results of numerical modeling of realization history of the potential for HC generation by different probably source formations of the East Barents Sea Basin are shown in Table 1 and Table 2. Here it are demonstrated age (t), depth (Z), temperature (T) and maturation level of OM in the present day sedimentary section of the Basin. In addition, the initial potential (HI), realization of this potential to the present time (Ht), integral volume of generated liquid (Ho) and gaseous (Hg) HC, time of entering of the rock into the "oil window" (t1) (Ro ≥ 0.50%) and exiting from it (t2) (Ro ≥ 1.30%), and, finally, the time of reaching of the expulsion threshold for liquid HC. Figure 13 and Figure 14 demonstrate change in integral volume of generated HC during burial history of the formations.

Our modeling assumes that the depositions of the Upper and Middle Triassic can be considered as source rocks for gas-condensate accumulations in the Ludlov, Shtockman and Ledovaya areas, where low organic matter content can compensate significant thickness of depositions. In turn, a degree of realization of hydrocarbon potential in the Jurassic and Cretaceous rocks in the Shtockman area was not enough to overcome an expulsion threshold (in our determination). Thus, formation of the oil accumulation in this area, generated by the rocks of the Upper Triassic and Lower Jurassic, is improbable. At the same time, the Jurassic and Cretaceous horizons contain the structures with accumulative and screening attributes needed to formation of gas and gas-condensate fields generated in the underlying Triassic layers.

Conclusion

The main inferences from the results of our modeling are integrated in Figure 15 and Figure 16 and Table 1 and Table 2. Variations in temperature and katagenesis of sedimentary rocks with depth are shown along the profile across the Admiralteyskoe Rise (Figure 15) and the profile along the axis of the East Barents Sea rift from Ludlov to Arctic areas (Figure 16). Relatively high temperature and maturation regimes are typical for the study region. These temperatures promoted significant thermal transformation of deep sedimentary rocks.

The liquid HC generated by the rock at the base of the Middle Devonian was destroyed to gas and coke if migration from these layers to the horizons with lower temperatures was absent (Figure 15 and Figure 16). In the case when the emigration took place, formation of HC accumulation must be at the depth no more 4-5 km. Such events are very improbable excluding perhaps the Pakhtusov and Admiralteyskaya areas. Consequently, the Devonian formations can be considered mainly as gas prone that is confirmed by depth of Ro-isolines in Figure 15 and Figure 16.

For the rocks in the base of the Permian in the Arctic, Shtockman, Ludlov, Ledovaya and even Krestovaya areas, the situation is just similar to the Devonian rocks and corresponding rocks can be considered as gas prone. In the Pakhtusov and Admiralteyskaya areas with lesser sedimentary thickness, the Low Permian rocks were oil prone for a long time (up to Upper Cretaceous). Now, gas generation consists less than 30% in total HC generation at present time; Table 1) Then, the Permian source rocks in the Pakhtusov and Admiralteyskaya areas could form the oil accumulations during the Cretaceous and Cenozoic provided that there were available collectors and covers and were the factors prevented a destroyed action of the Cretaceous and Cenozoic erosion. The Carboniferous and partly Upper Devonian rocks in the Pakhtusov and Admiralteyskaya areas remain mainly oil generating even up to present time and the Permian rocks are intensive generating oil by maturation level (Table 1 and Table 2).

The Triassic rocks at the depth of more than one kilometer in the Admiralteyskoe Rise are within the oil windows (Ro > 0.50%), and in the Admiralteyskaya area these rocks are characterized by Ro near 1% and by maturation can be considered as intensive oil generating (Table 1; Figure 3 and Figure 10). The Lower Triassic rocks in the Krestovaya area have high level of catagenesis with total destruction of liquid HC due to secondary creaking, whereas the Middle Triassic rocks are in the "window" (Table 1). However, these rocks are characterized by low OM content (Corg = 0.4%) and low initial potential for HC generation that can limit its possibility to form the HC accumulations. In the Ludlov, Ledovaya, Stockman and Arctic areas, the thickness of the Triassic rocks reaches 6-7 km and maturation level of OM ranges from overmature in the base of the formation to immature at the its roof (Table 2). Therefore, by generating potential, it is possible to form liquid HC accumulations by the Middle and Upper Triassic source rocks. Low Corg restricts strongly this possibility. As said above, some perspective can be related with the Jurassic rocks which in the Arctic area realize significant part of the HC potential and are characterized by rather high OM content (Corg is nearly 3%; Table 2).

The above numerical analysis implies that liquid HC generated by all rocks that occurred at high temperatures (T ≥ 140-160°C) and possessed high maturation of OM (Ro ≥ 1.20%), was subjected (possibly partly) to secondary creaking. It is typical for the Ordovician, Silurian, and Devonian deposits in the Admiralteyskaya and Pakhtusov areas (Figure 13 and Figure 14; Table 1 and Table 2) and for the Devonian, Permian and significant part Triassic deposits in the other considered areas (Figure 15 and Figure 16; Table 1 and Table 2). According to the modeling, in the present-day section of the Admiralteyskaya and Pakhtusov areas, the Carboniferous Permian, and Lower Triassic rocks at the depth from 1,000 to 4,000 m are the rocks generated oil, whereas deeper horizons are predominantly the gas prone rocks (Table 1 and Table 2).

The Ordovician, Silurian and Lower Devonian formations entered to the "oil window" at the Upper Devonian – Carboniferous and exit from this "window" in the Triassic, whereas the Frasnian rocks entered into the "oil window" in the Upper Permian and exit from it in the Upper Triassic (Table 1 and Table 2). In the present-day sections of the southern areas (the Ledovaya, Stockman and Arctic areas), the Triassic rocks at the depth of 2,500 - 4,200 m are the oil generating (Figure 16, Table 2). In these areas, the rocks at deeper horizons are predominantly gas-prone. The Lower Devonian formations in the southern areas entered to the "oil window" at the Carboniferous-Permian and exit from this "window" in the Permian-Triassic, whereas the Lower Triassic rocks entered into the "oil window" in the Middle Triassic and exit from it in the Upper Triassic (Table 1 and Table 2). As whole, the modeling suggests good perspective northern areas of the East Barents Basin to form oil accumulations, whereas in the southern areas HC accumulations must be predominantly gaseous.

References Cited

Applonov S.V., 2000, Geodynamics of the deep sedimentary basins: S.-P. TsGI TETIS, 214 p., (in Russian).

Bayer, A.J., 1981, Geotherms evolution of the lithosphere and plate tectonics: Tectonophysics, v. 72, p. 203-227.

Bogdanov, N.F. and Khain V.E., 1996, Remarks to tectonic map of the Barents Sea and northern part of the European Russia. Map and geological-geophysical profiles: The RAN Lithosphere Institut, 94 p.

Burnham, A.K., and R.L. Braun, 1990, Development of a detailed model of petroleum formation, destruction, and expulsion from lacustrine and marine source rocks, *in* B. Durand and F. Behar, eds., Advances in organic geochemistry 1989; Part 1, Organic geochemistry in petroleum exploration: Organic Geochemistry, v.16/1-3, p.27-39.

Burnham, A.K., and J.J. Sweeney, 1989, A chemical kinetic model of vitrinite maturation and reflectance: Geochimica et Cosmochimica Acta, v. 53/10, p. 2649-2657.

Carlslaw, H.S., and J.C. Jaeger, 1959, Conduction of heat in solids: New York, Oxford University Press, 386 p.

Espitalie, J., P. Ungerer, I. Irvin, and E. Marquis, 1988, Primary cracking of kerogens. Experimenting and modelling C1, C2-C5, C6-C15 classes of hydrocarbons formed: Organic Geochemistry, v.13/4-6, p. 893-899.

Forsyth, D.W. and F. Press, 1971, Geophysical tests of petrological models of the spreading lithosphere: Journal of Geophysical Research, v.76, p. 7963-7972.

Frakes, L.A., 1979, Climates throughout geological time: Elsevier, Amsterdam, p. 1-310.

Galushkin, Y.I., and Y.B. Smirnov, 1987, Thermal history of sedimentary basins: express-methods of heat flow assessment: Geologiya I Geophizika, v. 11, p.105-112. (in Russian).

Galushkin, Y.I., 1997a, Numerical simulation of permafrost evolution as a part of basin modeling: permafrost in Pliocene-Holocene climate history of Urengoy field in West Siberian basin: Canadian Journal of Earth Science , v.34/7, p. 935-948

Galushkin, Y.I., 1997b, The thermal effect of igneous intrusive bodies on maturity of organic matter - A possible mechanism of intrusion formation: Organic Geochemistry, v. 27/11-12, p. 645-658.

Galushkin Y.I., and G.E. Yakovlev, 2004, Burial and thermal history of the West Bashkirian sedimentary basins:Tectonophysics, v. 379, p. 139-157.

Galushkin, Y.I., KA. Sitar, and S.V. Frolov, 2013, Basin modeling of temperature and heat flow distributions and permafrost evolution, Urengoy and Kuyumbinskaya areas, Siberia: Permafrost and Periglacial Processes, v24/4, p. 1-17.

Galushkin, Y., E. Salim, and M. Sak, 2014, Burial and thermal history modelling of the Murzuq and Ghadames Basins (Libya) using the GALO computer programme: Journal of Petroleum Geology, v. 37/1, p. 69-92.

Golmshtock, A.Y., 1979, Effect of sedimentation on heat flow: Okeanologia, v.19/6, p. 1133-1138. (Russian).

Golmshtock, A.Y., 1981, Heat flow due to heat flow during sedimentation: Okeanologia, v. 21/6, p.1029-1033. (Russian).

Gramberg, I.S., 1997, The Barents Sea Permian-Triassic paleorift and its significance for oil-gas bearing problems in the Barents Karskoe plate: Doklady RAN, T., v. 352/6, p. 789-791. (Russian).

Gramberg, I.S., N.K. Evdokimova, and O.I. Suprunenko, 2001, Catagenesis zoning of sedimentary blanket of the Barents Sea shelf in relation with the oil and gas prospecting of the region: Geologiya I Geophizika, v. 42/11-12, p. 1808-1820. (Russian).

Khutorskoy, M.D., and L.V. Podgorny, 2001, Three-dimensional model of geothermal field of the Barents Sea region: Doklady RAN, v. 377/1, p. 96-100. (Russian).

Kogan, L.I., and R.R. Murzin, 1997, The East Barents Sea depression is the one of ancient in the Earth (according to seismic data):"Geologia morey I okeanov: XII International geological school, Abstracts ", v.1, GEOS, p. 253-254. (Russian).

Kogan, L.I., Y.P. Malovitskiy, and R.R. Murzin, 2002, Deep structure of the East Barents depression by the data of wide angle seismic sounding: Razvedka I Okhrana Nedr, v. 8, p. 52-58. (Russian).

Korotaev M.V., A.M. Nikishin, E.V. Shipilov, S. Cloetingh, and R.A. Stefenson, 1998, Geological history of the East Barents Sea region in the Paleozoic-Mesozoic by the data of computer modeling: Doklady RAN, v. 359/5, p. 654-658. (Russian).

Levashkevich V.G., 2005, Patterns in geothermal field distribution over the East-European platform edges (Barents and Byelorussia-Baltic regions): PhD thesis, Moscow University, Moscow, 42 p.

Makhous, M., Y.I. Galushkin, and N.V. Lopatin, 1997, Burial history and kinetic modelling for hydrocarbon generation. Part I: The GALO Model: AAPG Bulletin, v. 81/10, p. 1660-1678.

Makhous, M., and Y.I. Galushkin, 2003, Burial History and Thermal Evolution of the Lithosphere of the Northern and Eastern Saharan Basins: AAPG Bulletin, v. 87/10, p. 1623-1651.

Makhous, M., and Y. Galushkin, 2005, Basin analysis and modeling of the burial, thermal and maturation histories in sedimentary basins: Paris, Editions TECHNIP, 380 p.

Neprochnov, Y.P., G.A. Semonov, N.V. Sharov, J. Yliniemi, K. Komminaho, U. Luosto, and P. Heikkinen, 2000, Comparison of the crustal structures of the Barents Sea and the Baltic Shield from seismic data: Tectonophysics, v. 321, p. 429-447.

Perrier, B., and J. Quiblier, 1974, Thickness changes in sedimentary layers during compaction history: methods for quantitative evaluation: AAPG Bulletin, v.58/3, p.507-520.

Podgorny L.V., and M.D. Khutorskoy, 1998, Thermal evolution of the lithosphere in the zone of joint of the Baltic shield and the Barents Sea plate: Phizika Zemli, v. 4, p. 3-9. (Russian).

Shipilov E.V., and A.P. Mossur, 1990, Anomalous seismic horizons in the sedimentary cover of the Barents Sea: Geotectonica, v. 1, p. 90-96. (Russian).

Sweeney, J.J., and A.K. Burnham, 1990, Evolution of a simple model of vitrinite reflectance based on chemical kinetics: AAPG Bulletin, v.74/10, p. 1559-1570.

Tissot, B.P., R. Pelet, and P. Ungerer, 1987, Thermal history of sedimentary basins, maturation indices, and kinetics of oil and gas generation: AAPG Bulletin, v.71/12, p. 1445-1466.

Tsybulya, L.A., and V.G. Levashkevich, 1992, Heat flow in the Barents Sea region: Appatite, 114 p. (Russian).

Tsybulya, L.A., 1993, Geothermal conditions in the Barents-Karsky region and their influence on formation of oil and gas accumulations, in V.P. Gavrilov, ed., Geodynamics and oil and gas bearing in Arctic: M., Nedra, p. 146-159 (Russian).

Turcotte D.L., and G. Schubert, 1982, Geodynamics: John Wiley and Son, 374 p.

Ungerer, P., I. Burrus, B. Doligez, P. Chenet, and F. Bessis, 1990, Basin evolution by integrated two-dimensional modeling of heat transfer, fluid flow, hydrocarbon generation, and migration: AAPG Bulletin, v. 74/3, p. 309-335.

Ungerer P., 1993, Modeling of petroleum generation and migration, *in* M.L. Bordenave, ed., Applied Petroleum Geochemistry: Technip, Paris, p. 397-442.

Velichko, A.A., ed., 1987, Climatic variations in Meso-Cenozoic by the data for East Europe *in* Climates of the Earth in geological history: Nauka, Moscow, p. 5-43. (Russian).

Velichko, A.A., ed., 1999, The climate and landscape during the last 65 Ma (Cenozoic: from Paleocene to Holocene): GEOS, Moscow, 260 p. (Russian).

Verzhbitsky E.V., 2000, Geothermal regime and origin of the eastern part of the Barents Sea region: Okeanologiya, v. 40/3, p. 448-455. (Russian).

Verzhbitsky E.V., 2002, Geothermal regime, floor tectonics and temperature conditions for HC generation in the eastern part of the Barents Sea: Geotectonica, v. 1, p. 86-96. (Russian).

Welte D.H., B. Horsfield, and D.R. Baker, eds., 1997, Petroleum and basin evolution: Springer-Verlag, 536 p.

Wyllie, P.J., 1979, Magmas and volatile components: American Mineralogist, v.64, p.469-500.

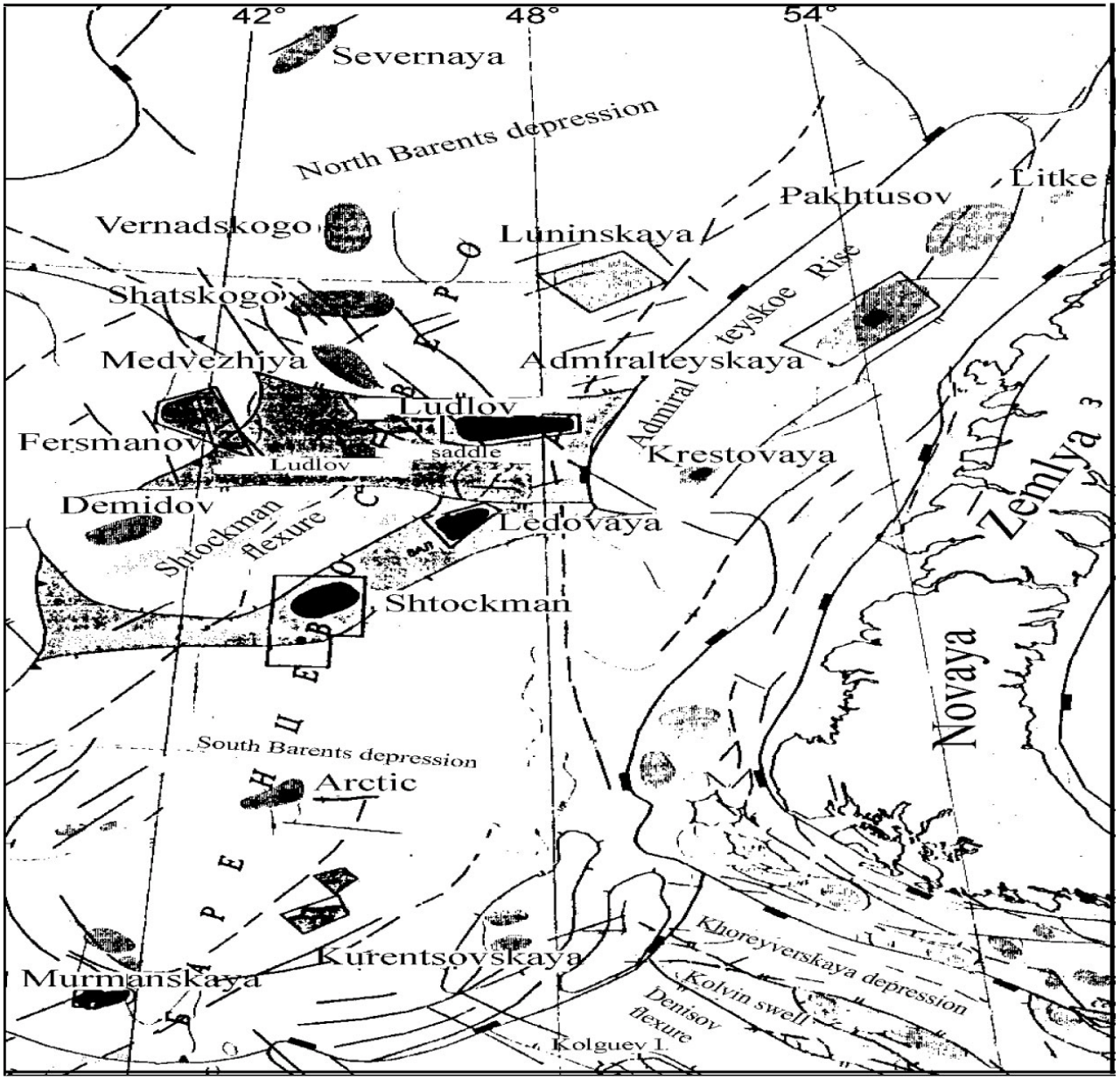

Figure 1. Location of the studied areas and the main tectonic structures in the East-Barents region.

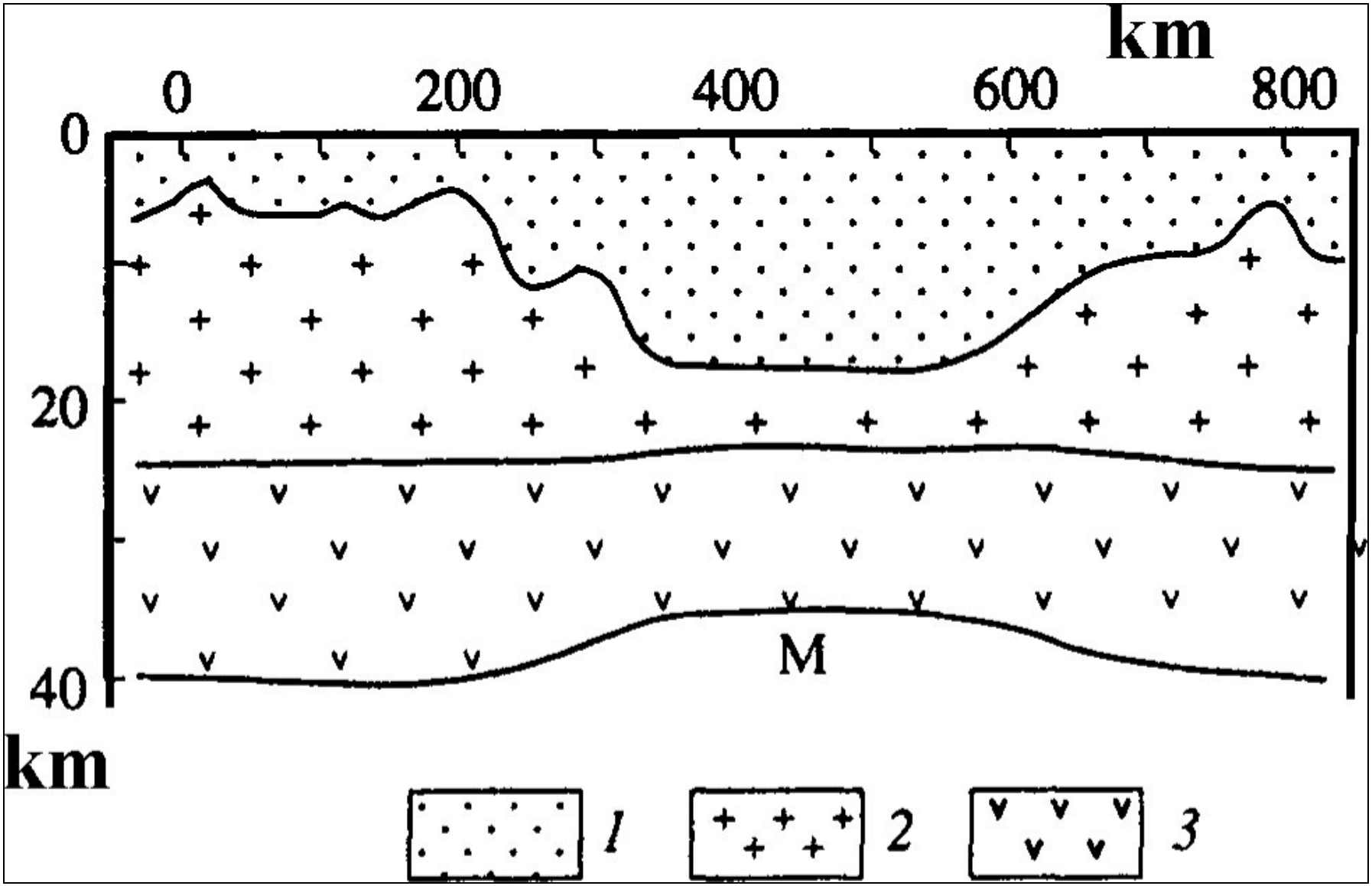

Figure 2. Cross-sections of the crust along the profile from west to east crossed the Ledovaya area. The section was constructed on the base of seismic and gravity data (Shipilov and Mossur, 1990). 1 – sediments; 2 – granite; 3 – “basalt”; M – Mohorovich boundary.

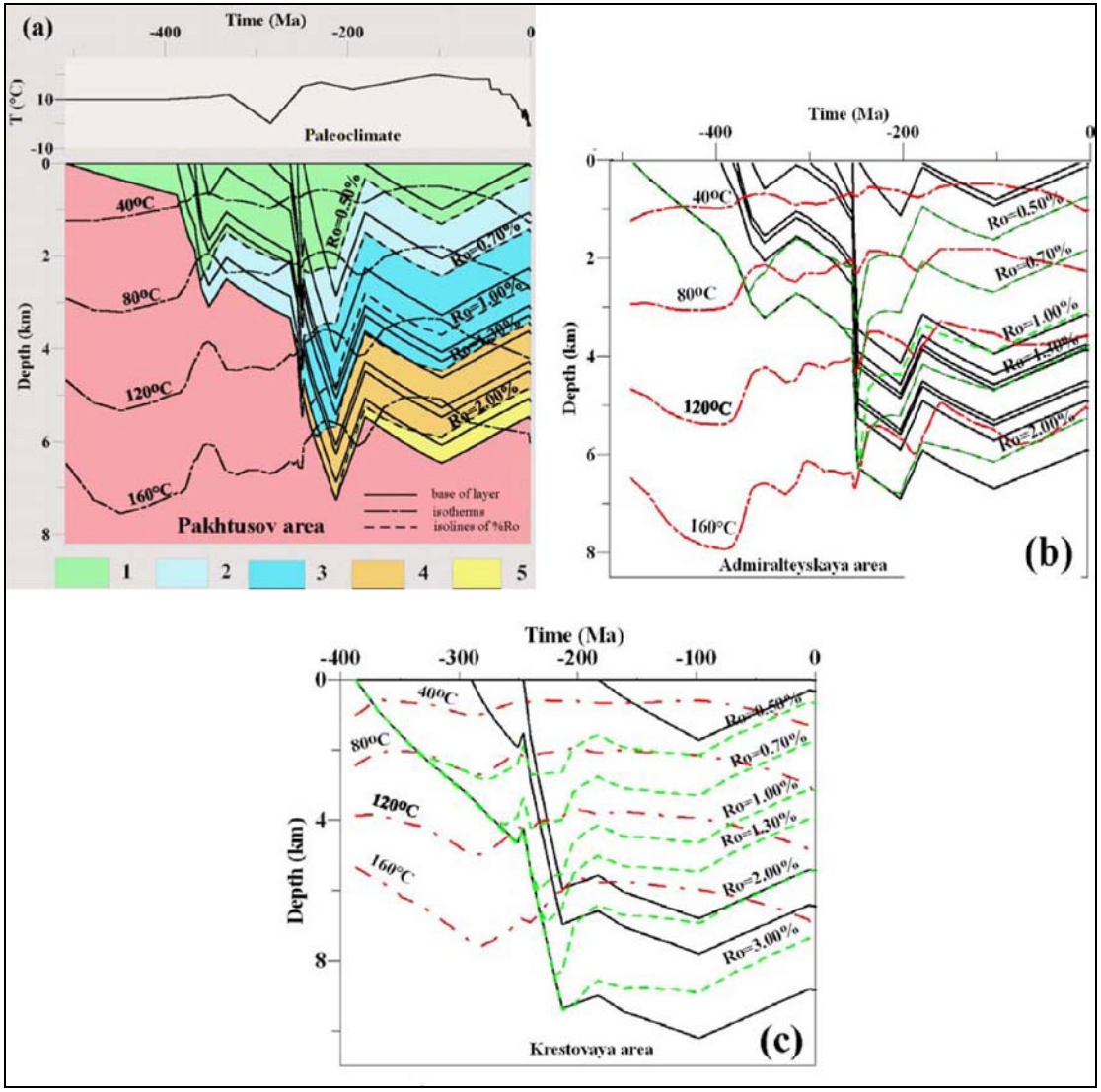

Figure 3. Burial and thermal evolution of sedimentary section of the East Barents Basin in the Pachtusov, Admiralteyskaya and Krestovaya areas of the Admiralteyskoe Rise (Figure 1). Legend in the right lower angle of (a). Isolines of vitrinite reflectance, Ro (%), are characterized maturation of sediment's organic matter. In (a): 1 – immature rocks (Ro ≤ 0.50%); 2 – start of oil generation (0.50% ≤ Ro ≤ 0.70%); 3 – the main zone of oil generation (0.70% ≤ Ro ≤ 1..30%); 4 – zone of wet gas generation (1.30% ≤ Ro ≤ 2.00%); 5 – dry gas generation (Ro ≥ 2.00%).

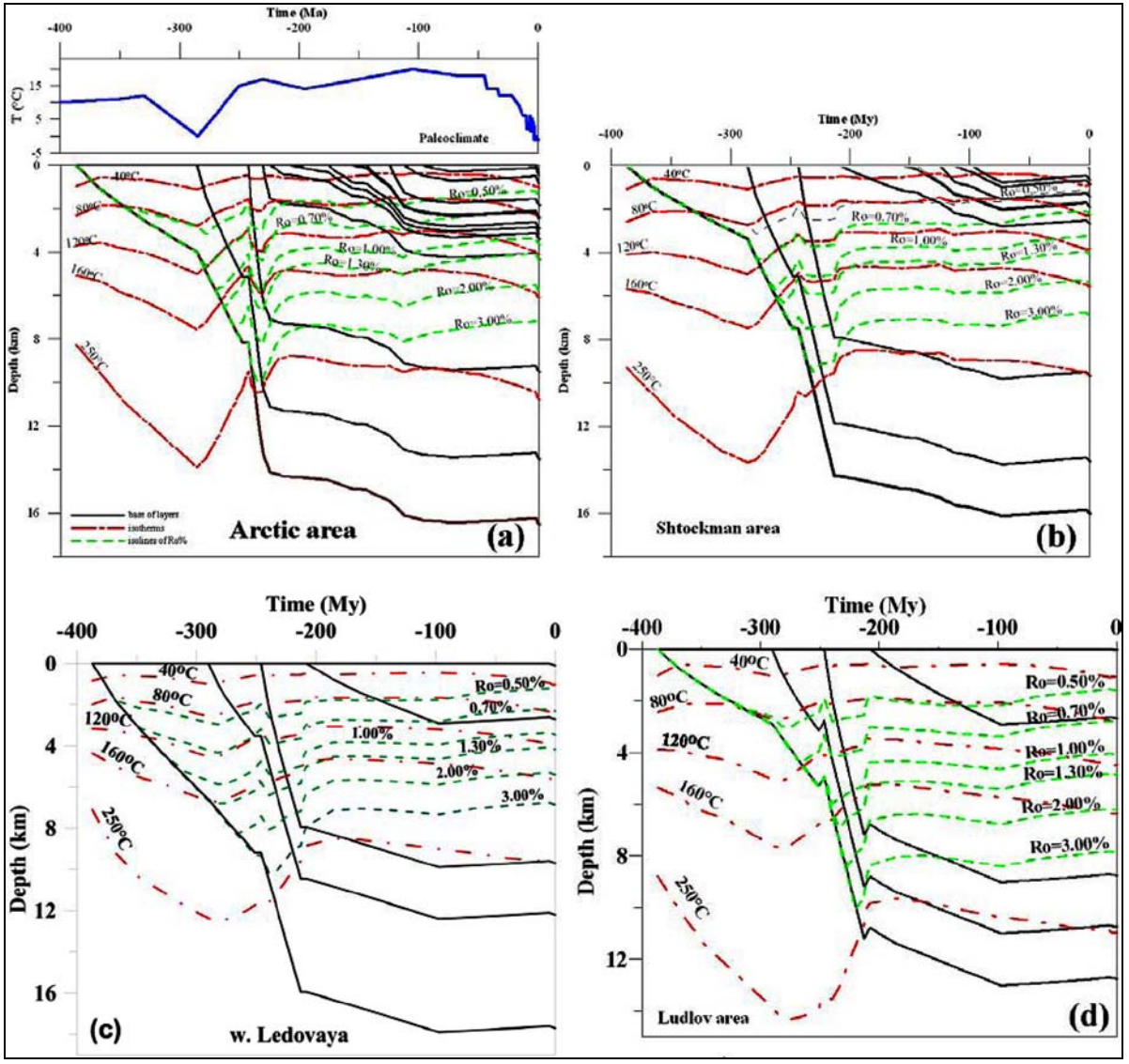

Figure 4. Burial and thermal evolution of sedimentary section of the East Barents Basin in the Arctic, Shtocman, Ledovaya and Ludlovskaya areas (Figure 1). Legend in the left lower angle of (a). Isolines of vitrinite reflectance, Ro (%), are characterized maturation of sediment's organic matter.

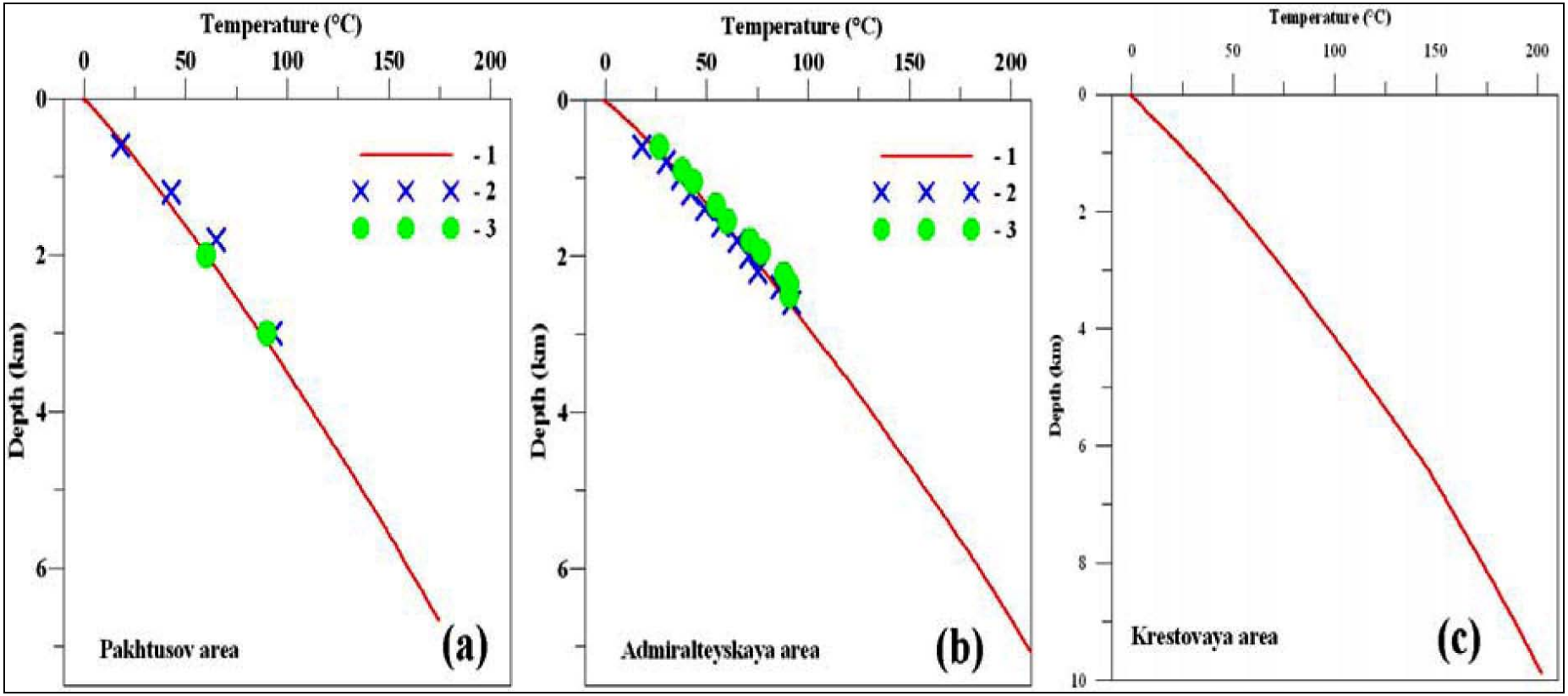

Figure 5. Calculated and measured temperatures in the present-day sections of the Pakhtusov, Admiralteyskaya and Krestovaya areas of the East Barents Sea Basin (Figure 1). 1 – temperature distribution calculated without consideration of detail climate variations during last three My. 2 - temperatures measured in sedimentary section of the Admiralteyskaya area (Tsybulya and Levashkevich, 1992), 3 in (b) – carotage data (private report, Zakharov E.V.) and 3 in (a) – approximate averaged assessments of temperature for the rocks of the Pakhtusov sedimentary section (Levashkevich, 2005).

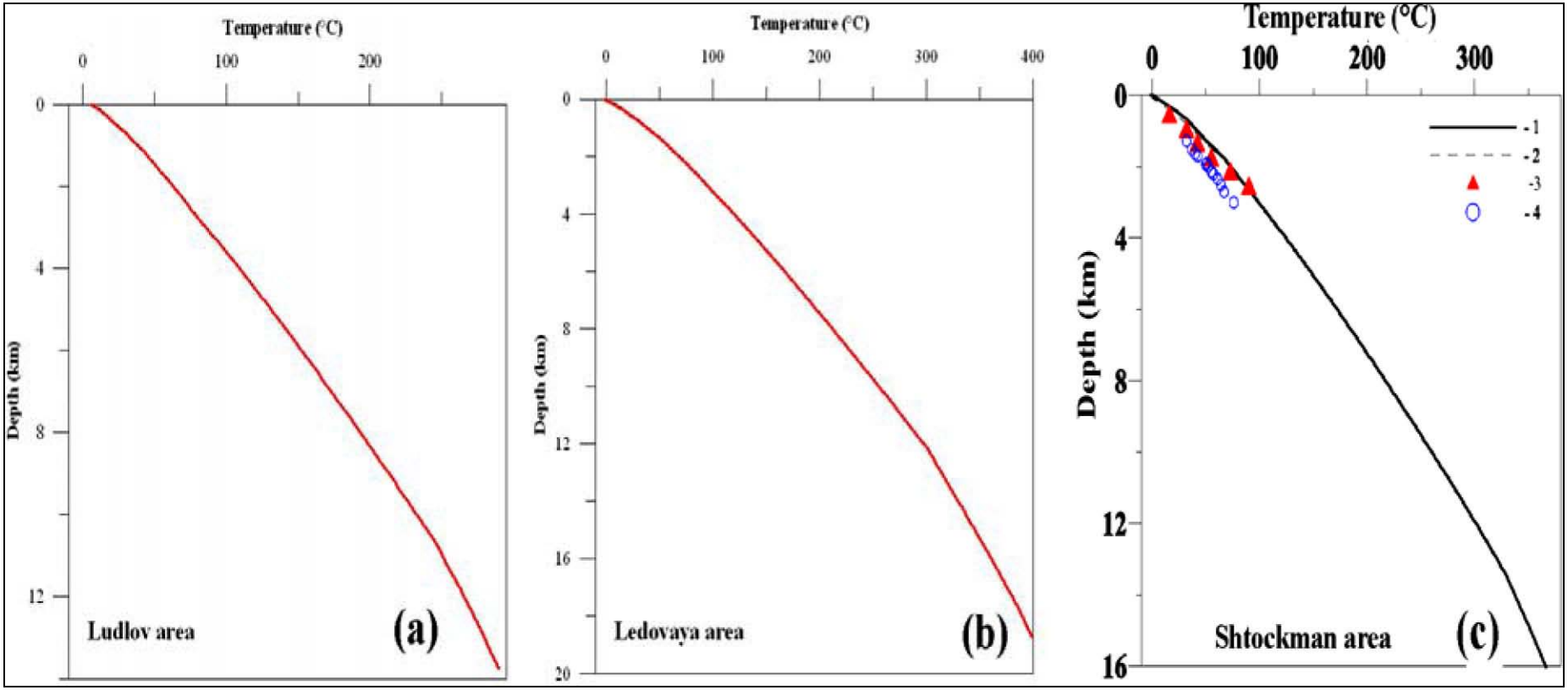

Figure 6. Calculated and measured temperatures in the present-day sections of the Ludlov, Ledovaya and Shtockman areas of the East Barents Sea Basin. (c): 1 – calculated temperatures, 3 – temperatures measured in the Arctic area; 4 – temperatures measured in Shtockman well, but with small time of staying after drilling (Tsybulya and Levashkevich, 1992).

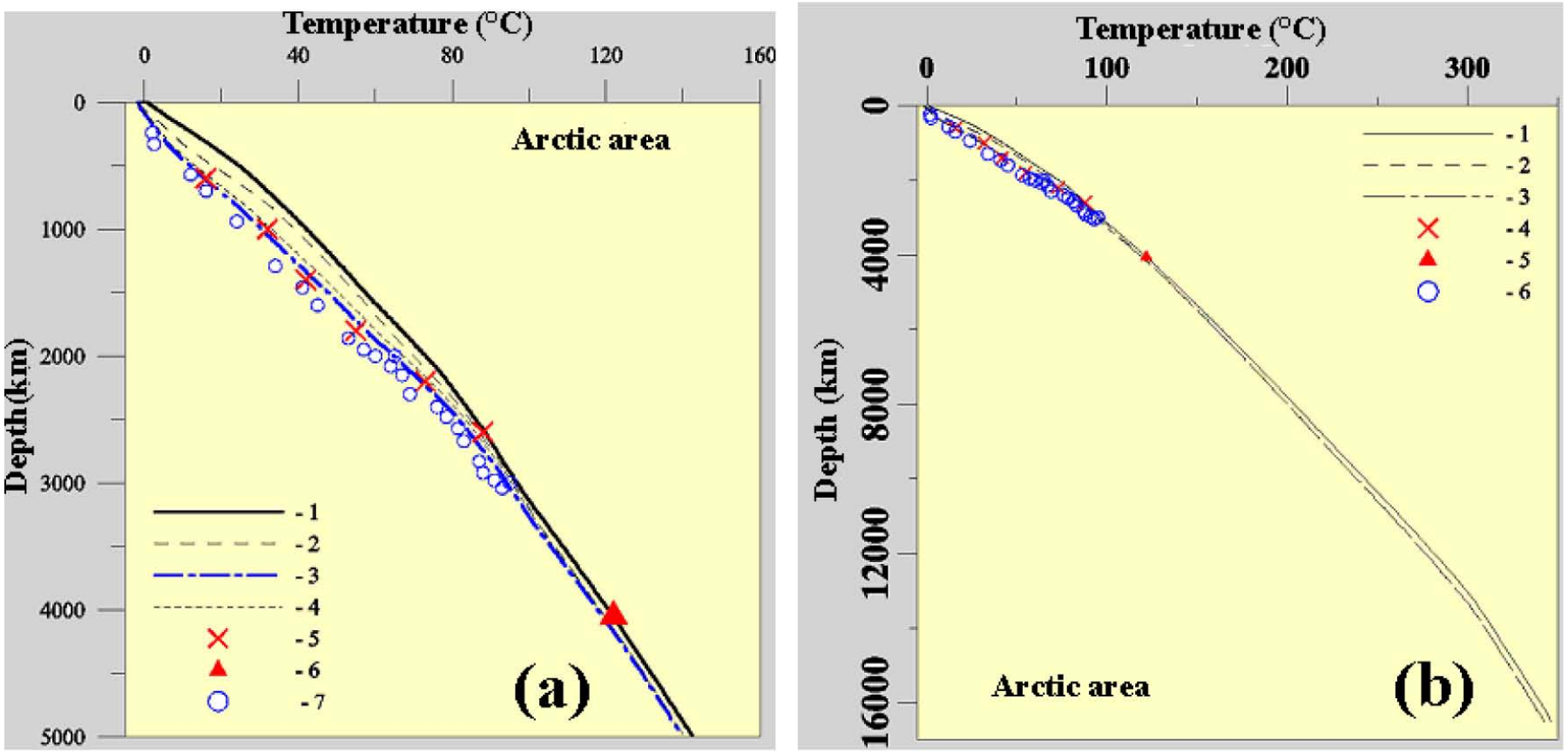

Figure 7. Calculated and measured temperatures in the present-day sections of the Arctic area of the East Barents Sea Basin.

1 – Profile computed with paleoclimate curve on upper part of Figure 4a.

2 – 4 in (a) and 2 in (b) – temperature profiles computed with detailed climate curves for the last 3 My by use of the special modification of the Galo system (Galushkin, 1997a). The salt content was adopted in calculations to be equaled to Csalt=15 g/litre.

2 – The surface temperature of the sedimentary cover during the coolest time of the Quaternary was given as T = -1.7°C (sea bottom).

3 in (a) – variant 2, but with T= -15°C during the coolest time of the Quaternary (80,000 < t < 15,000 years ago). By other words, freezing of the sea was assumed in this time.

4 in (a) – variant 2, but with surface temperature T= -15°C during the time period 50,000 < t < 15,000 years ago.

5 in (a) and 4 in (b) – measured values from the paper (Tsybulya and Levashkevich, 1992).

6 in (a) and 5 in (b) – measured formation temperatures (private report).

7 in (a) and 6 in (b) – measured values from (Levashkevich, 2005).

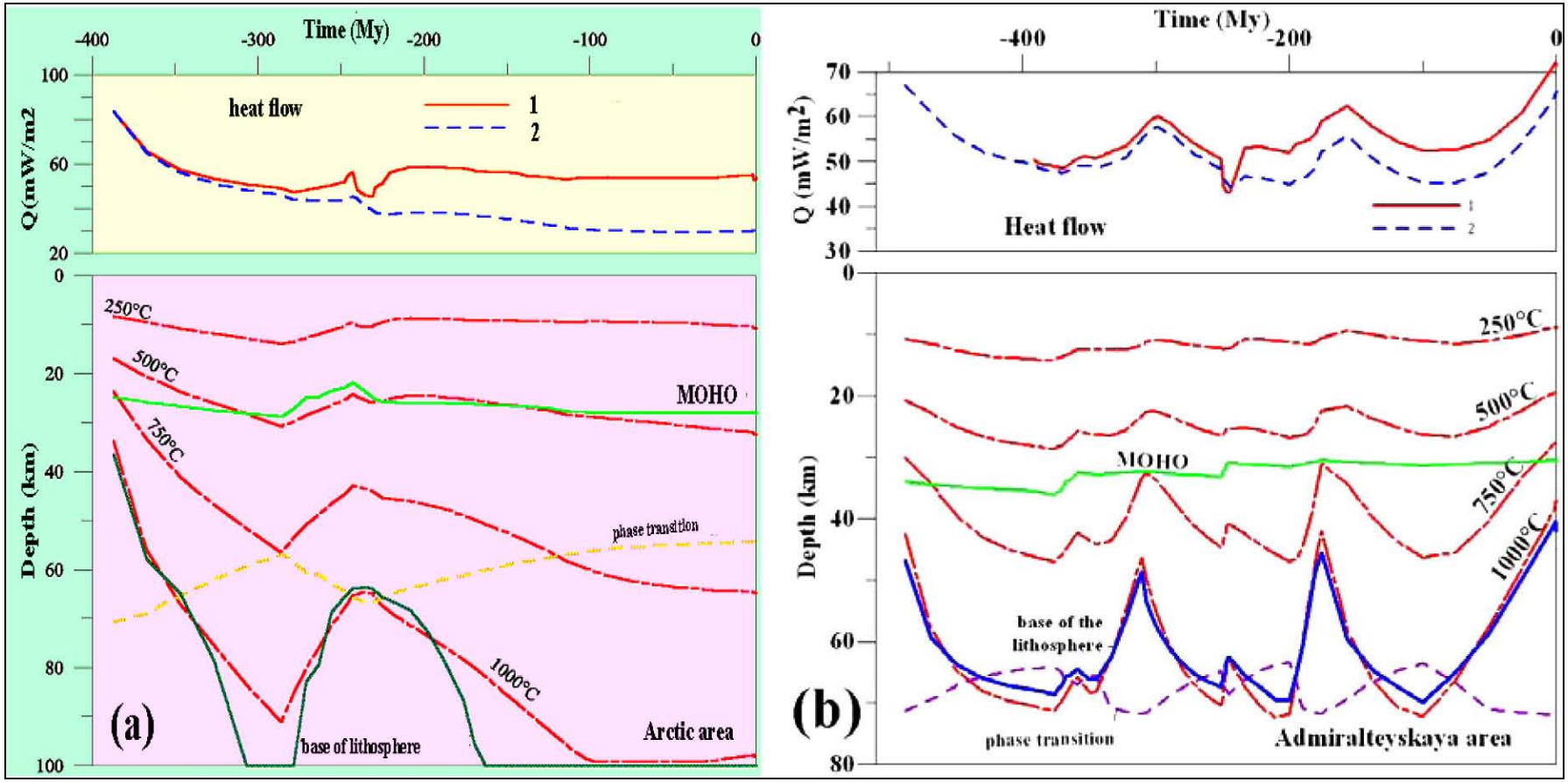

Figure 8. Thermal history of the basin lithosphere in the Arctic (a) and Admiralteyskaya (b) areas – numerical reconstructions in the GALO system. The figure demonstrates a higher heating of northern areas in comparison with the southern. Upper Figures: Calculated variation in heat flow. Distinction of heat flow through the basement surface (dotted line -2) from the one through the sediment surface (solid line – 1) is mainly due to the contribution of radiogenic heat of sediments. Lower Figures: Reconstruction of thermal history of the lithosphere. Blue solid line – the base of the lithosphere determined by intersection of the current geotherm with solidus of peridotite with 0.2% H_2O (Wyllie, 1979)). Long-dashed lines – isoterms. MOHO-line – base of the crust (the crust thickness increases during sedimentation and decreases during intensive extension of the lithosphere in the Permian-Triassic). The phase transition line shows the depth of phase transition spinel peridotite (ρ = 3.30 g/cm^3 at T = 0°C) to garnet peridotite (ρ = 3.38 g/cm^3; Forsyth and Press, 1971)

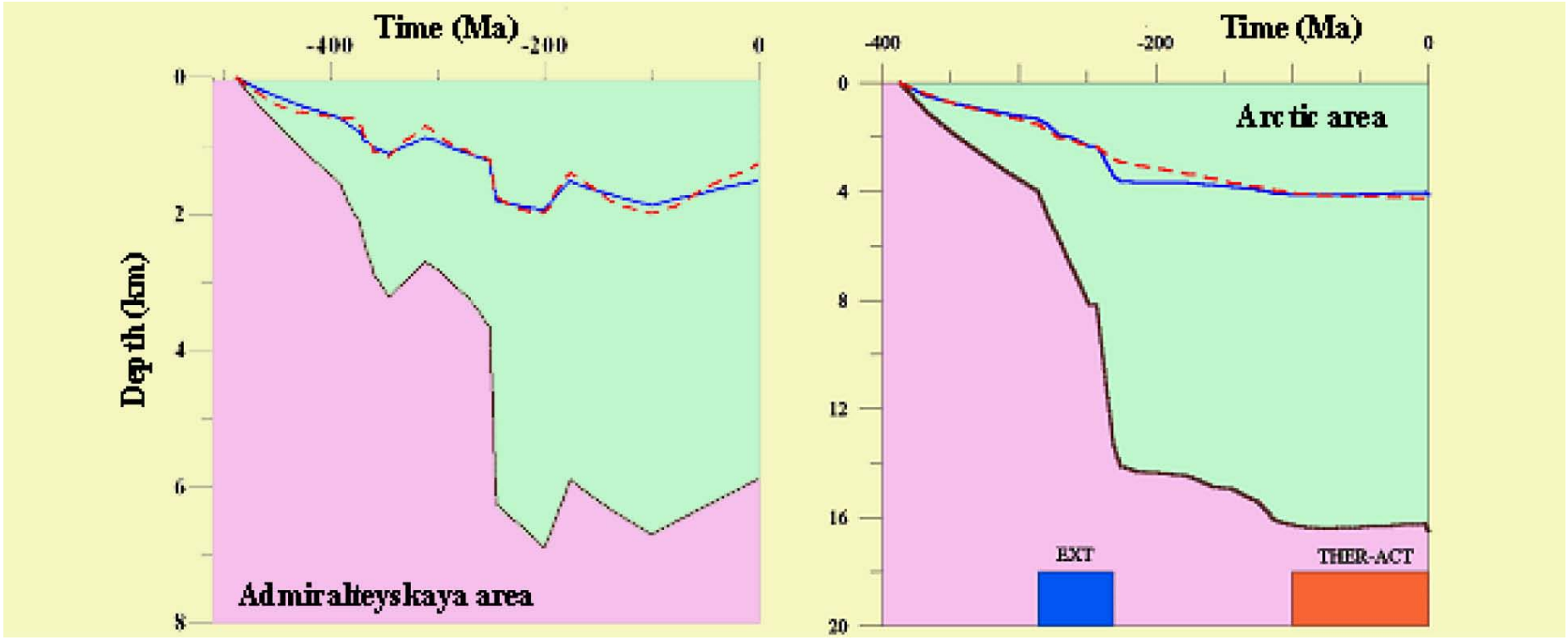

Figure 9. Tectonic subsidence of the basement surface in the Admiralteyskaya and Arctic areas of the East Barents Basin calculated in the local isostasy approach. Upper solid line - calculated by removing sediment and water load Upper dashed line – calculated by consideration of time-variations in density profile of the basement. Lower solid line – depth of the basement surface received by usual "backstripping" procedure ThER-ACT is the stage of thermal reactivations of the basin lithosphere in the Upper Cretaceous and Cenozoic, that prevented fast cooling of the lithosphere; EXT is the period of the lithosphere extension in the Permian-Triassic (see text).

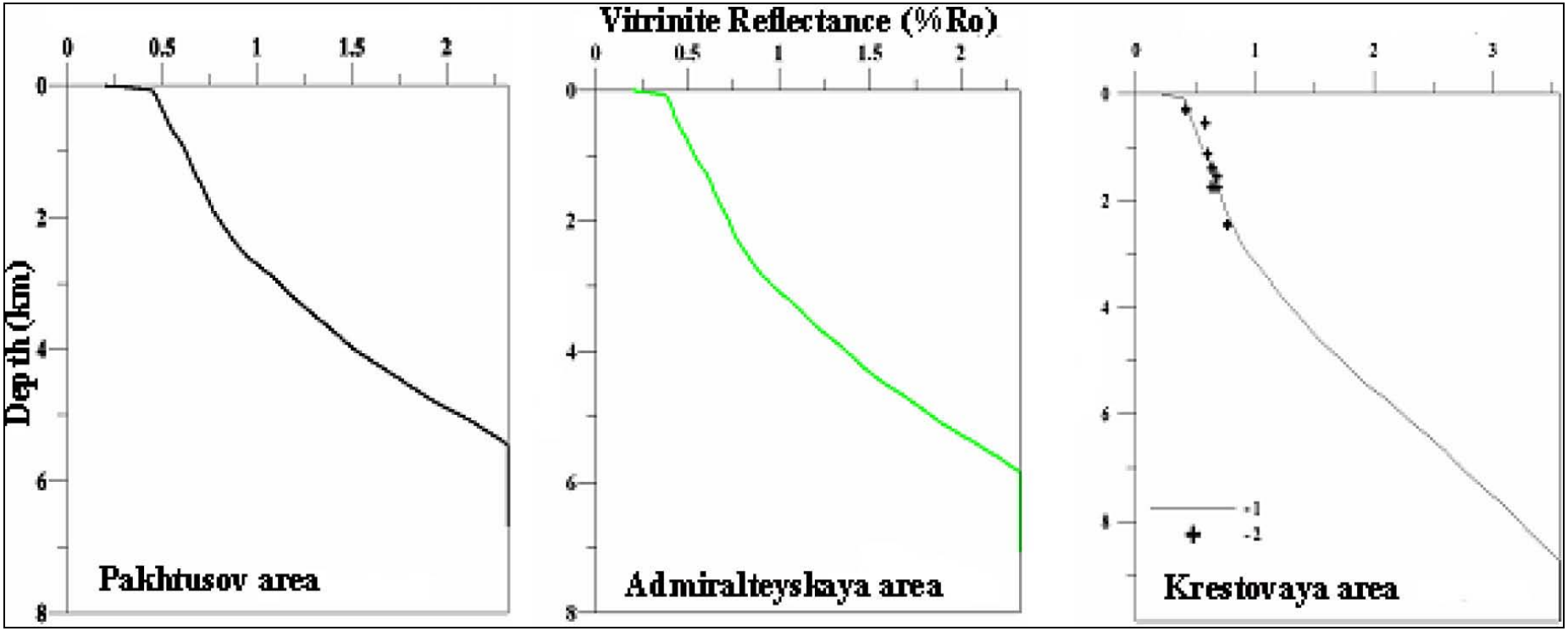

Figure 10. Distribution of vitrinite reflectance with depth in the areas of the Admiralteyskoe Rise. 1 – calculated, 2 – measured %Ro (Gramberg et al, 2001).

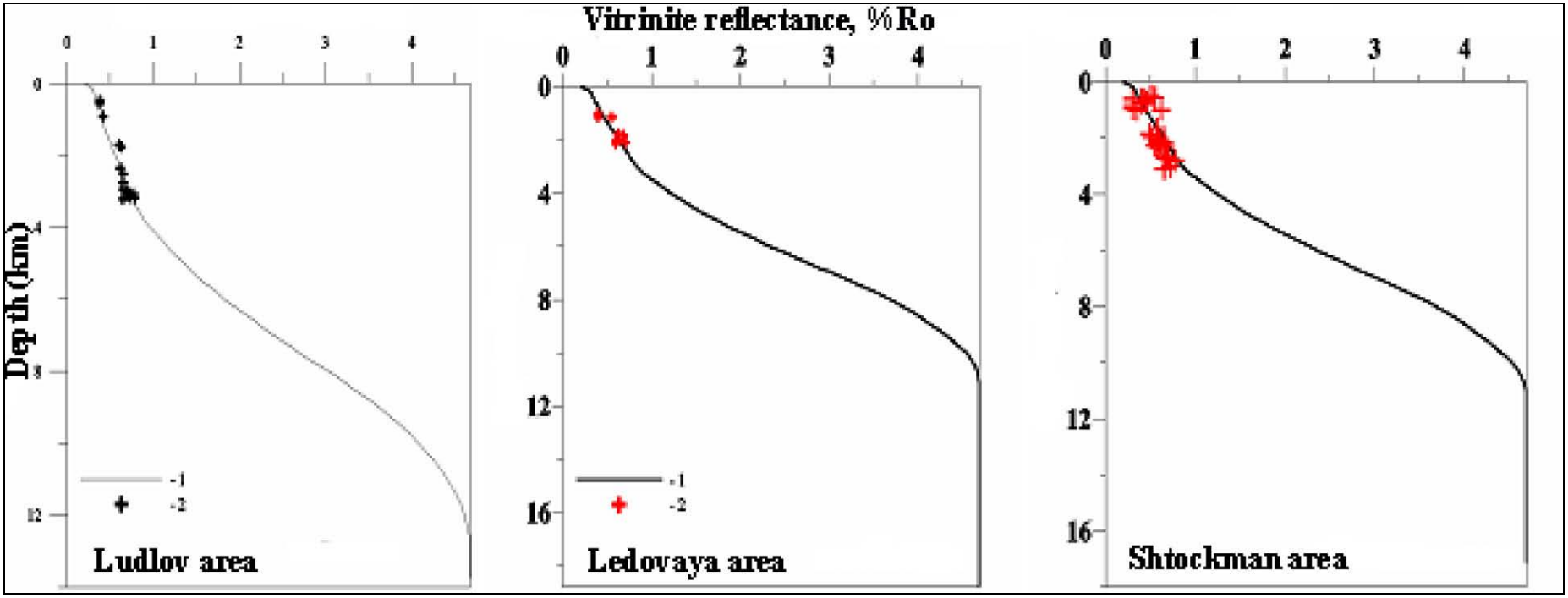

Figure 11. Distribution of vitrinite reflectance with depth in the Ludlov, Ledovaya and Shtockman areas. 1 – calculated, 2 – measured %Ro (Gramberg et al, 2001).

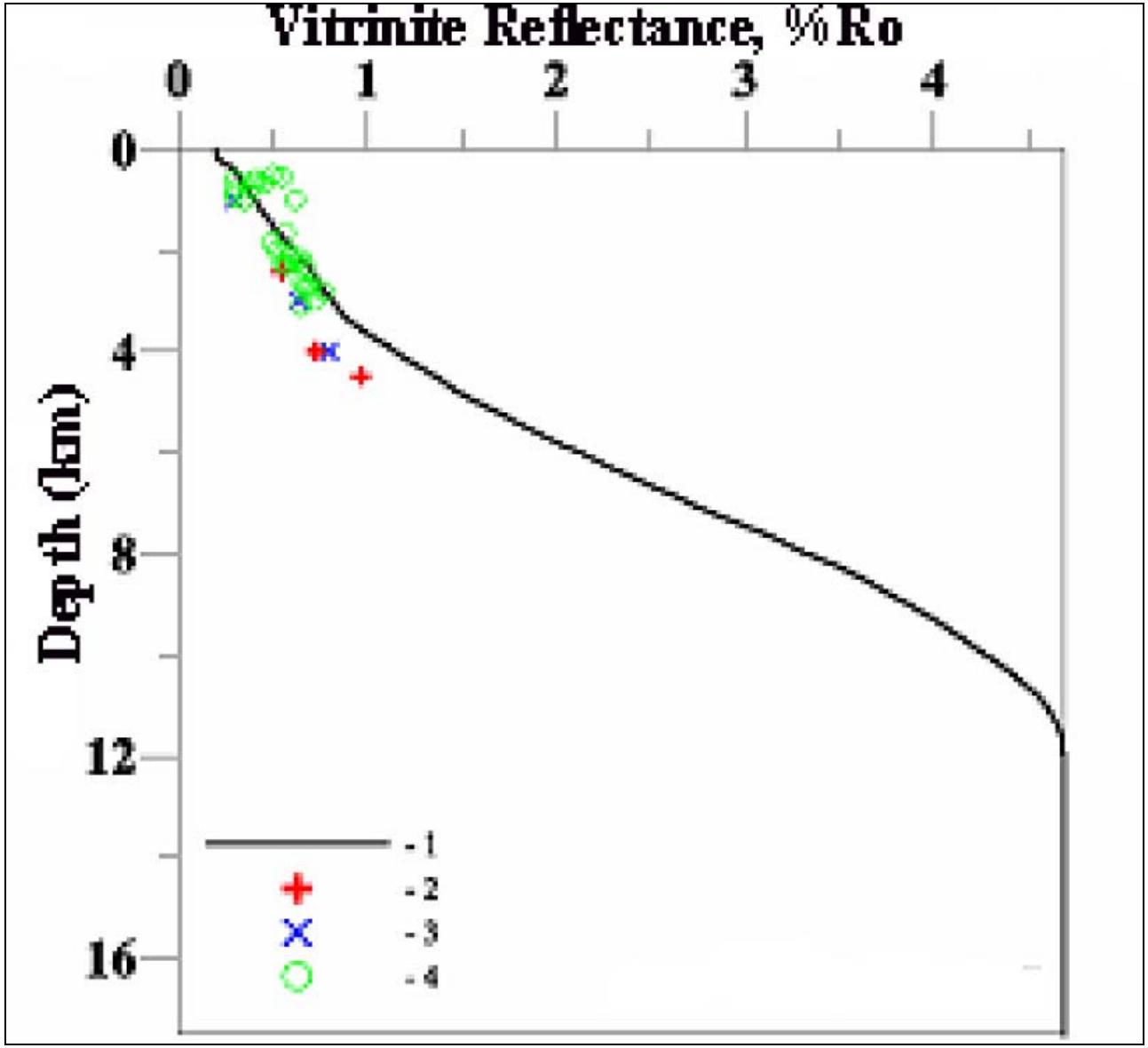

Figure 12. Distribution of vitrinite reflectance with depth computed for present-day section of in the Arctic areas using the GALO system. 1 – calculated %Ro, 2-4 – measured %Ro: 2 – private report; 3 – (Gramberg et al, 2001); 4 – scientific report (2002).

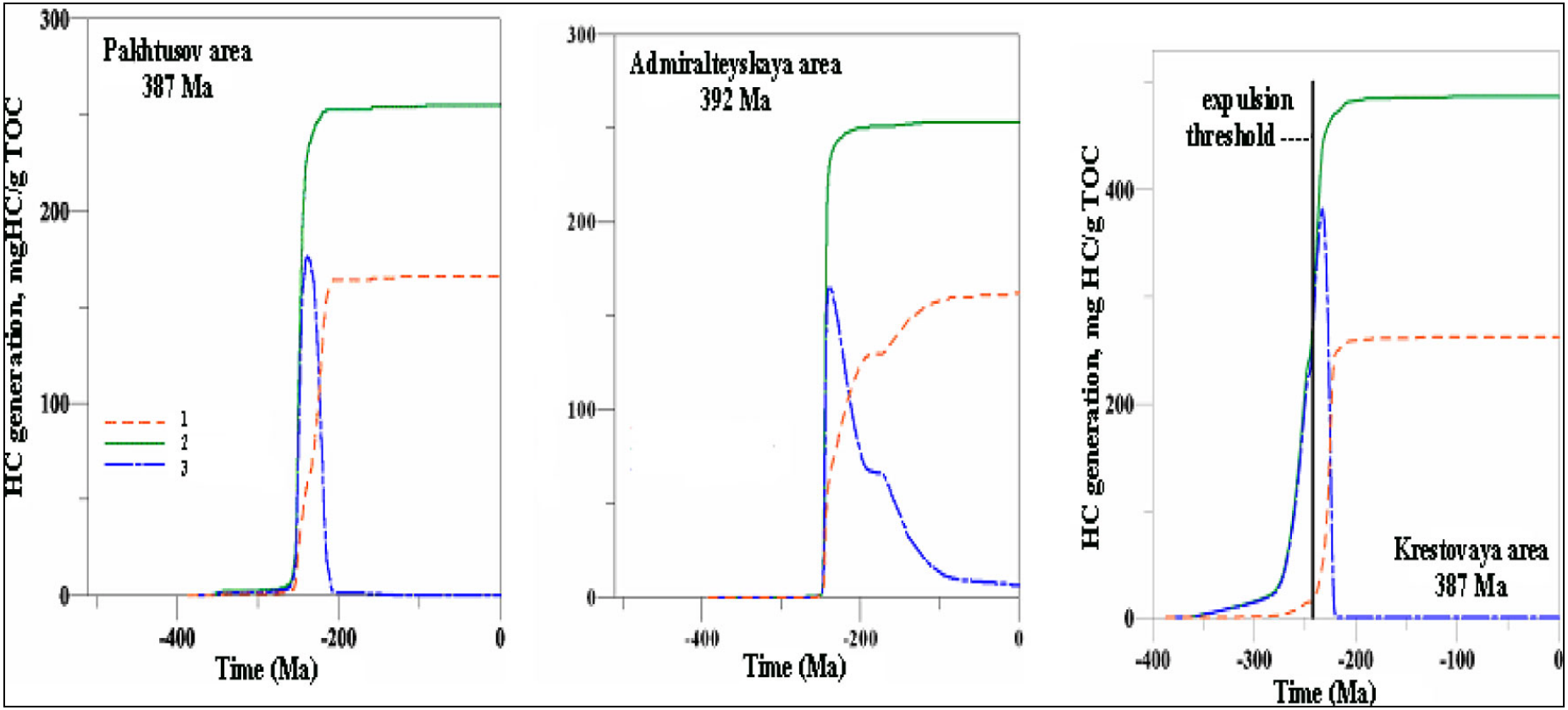

Figure 13. Realization of HC potential by the probably Devonian source formation during burial history of sedimentary cover in the Admiralteyskaya area of the East Barents Sea Basin. 1 – gaseous HC generation; 2 – total HC generation; 3 – liquid HC generation

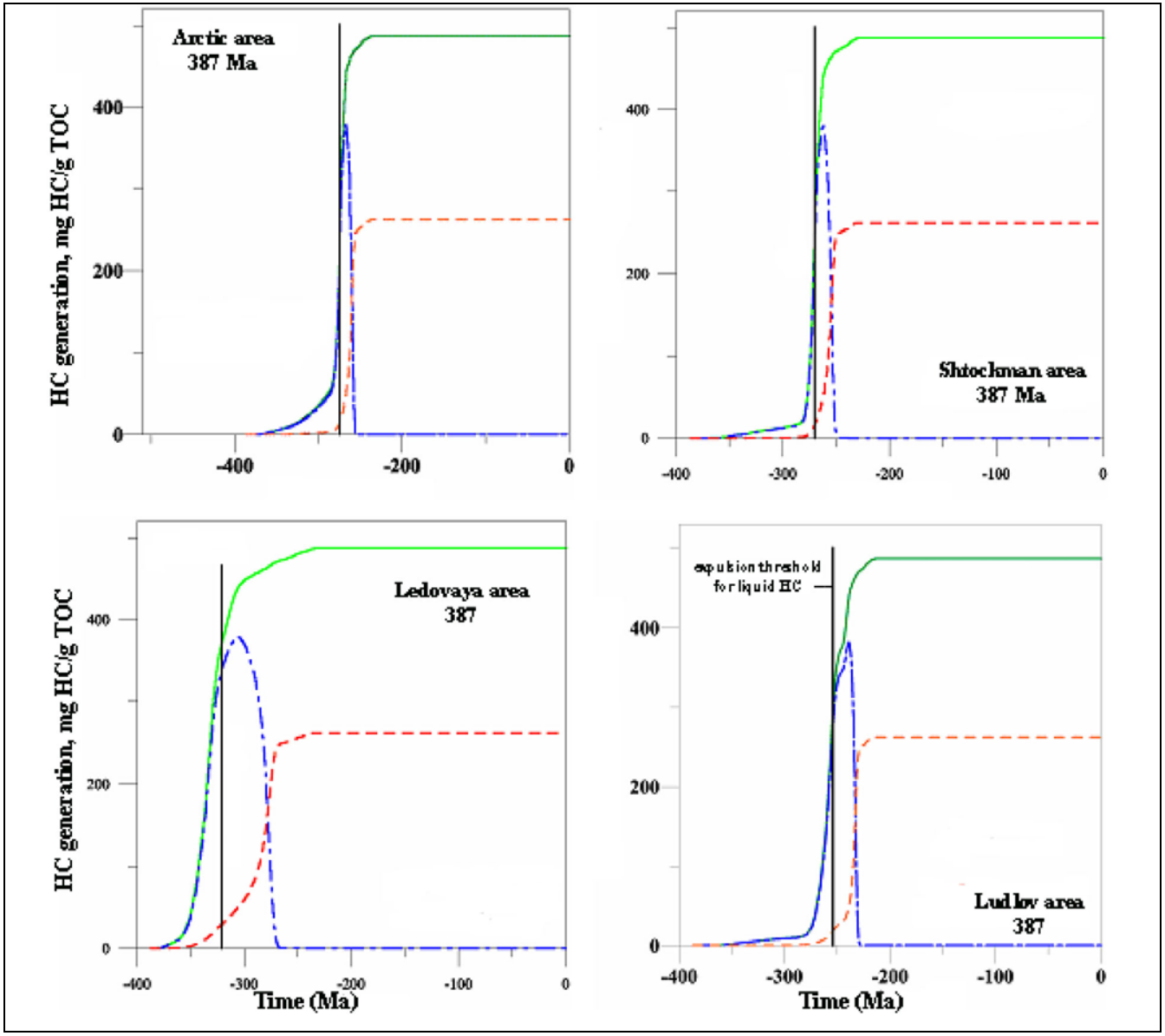

Figure 14. Realization of HC potential by the probably Devonian source formation during burial history of sedimentary cover in the southern part of the East Barents Sea Basin.

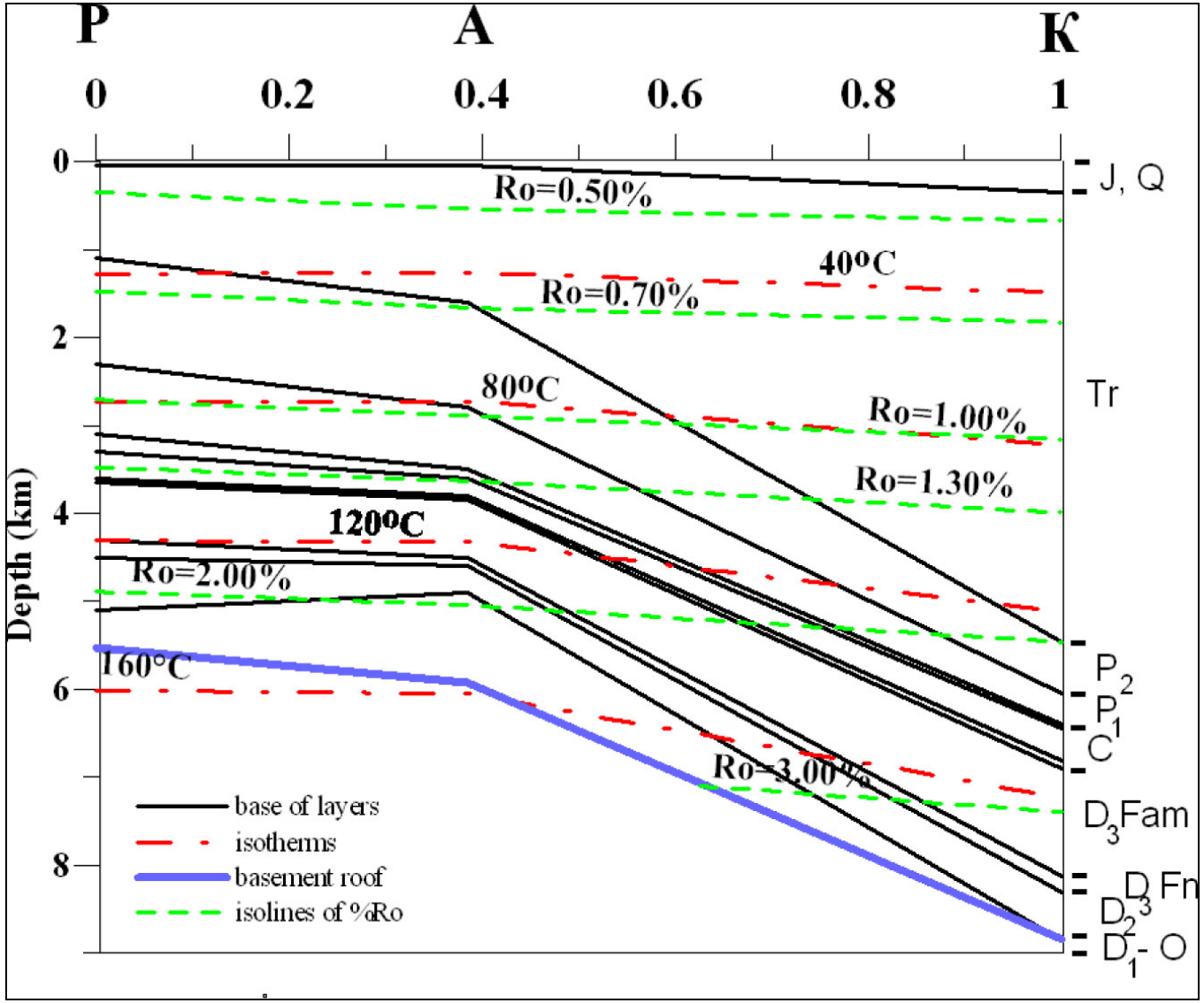

Figure 15. Distribution of rock temperature and OM maturation versus depth in the present day sedimentary section along the axis of the Admiralteyskoe Rise. P, A and K – approximate location of the Pakhtusov, Admiralteyskaya and Krestovaya areas in the profile. Simple linear interpolation was used between the areas under reconstruction to avoid additional errors.

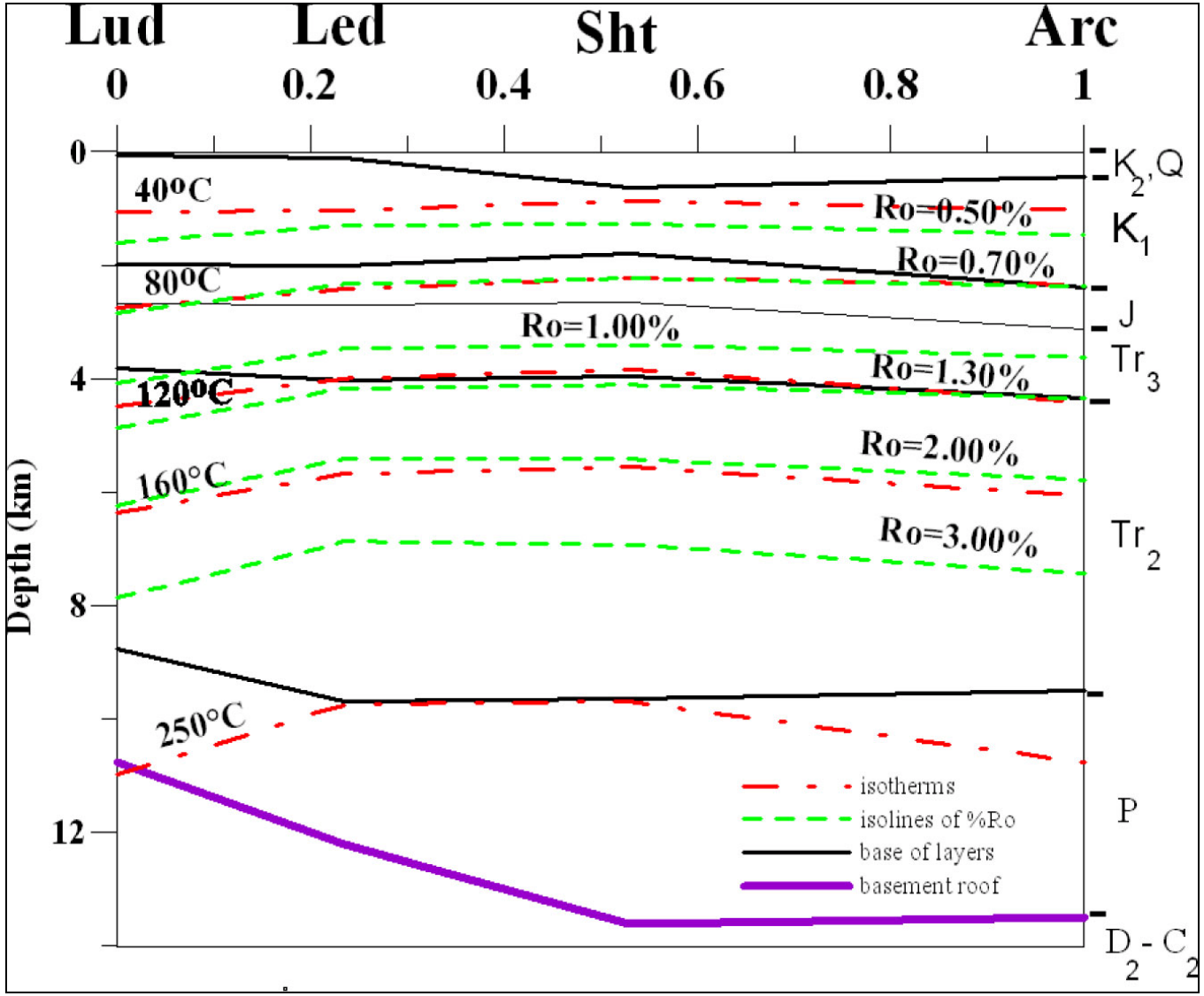

Figure 16. Distribution of rock temperature and OM maturation versus depth in the present day sedimentary section along the profile closed to the axis of the Devonian rift. Lud, Led, Sht, and Arc – approximate location of the Ludlovskaya, Ledovaya, Shtockman and Arctic areas in the profile. Simple linear interpolation was used between the areas under reconstruction to avoid additional errors.

T	Z	T	Ro	Hi	Ht	Ho	Hg	t1	texp	t2
My	m	°C	%	Mg HC/g Corg				Million years ago		
Pakhtusov area										
508	5500	147.4	2.306	377	377	0.	221	361	252	235
387	5100	138.2	2.090	268	255	0.035	166	357	-	230
374	4500	123.6	1.7749	668.5	664	324	182	265	248.7	222
367	4300	118.7	1.640	377	377	64.8	188	257	-	219
360	3650	102.7	1.354	377	377	252	94.8	252	-	119
286+	3300	94.1	1.200	377	377	293	74.3	250	-	-
286-	3300	94.1	1.200	268	238	161	71.6	250	-	-
263	3100	88.8	1.135	268	234	166	66.1	249	-	-
255	2300	67.7	0.857	268	168	128	40	240	-	-
248	1100	34.3	0.635	268	6.51	4.59	1.92	222	-	-
Admiralteyskaya area										
488	5900	180.6	2.306	377	377	0.	221	362	247	241
392	4900	154.5	1766	268	253	6.2	162	273	244	230
374	4500	143.6	1.558	668.5	662	388	151	249	245	217
359	3864	126.6	1.297	377	377	273	84	247	242	0
299	3764	123.8	1.253	377	377	284	79	246.5	241	-
271	3564	118	1.173	268	237	164	69.2	246	234	-
251	3138	105.6	1.014	268	223	164	59	245	222	-
Krestovaya area										
387	8850	184.7	3.553	487	487	0.	262	264	242.1	229
290	6450	145.4	2.439	619	614	0.003	331	232	228.3	216
246	5450	125.3	1.907	225.1	204	0.127	143	225	-	203
235	3350	83	1.070	225.1	171	112	58.2	213	-	-
223	1900	50.5	0.709	225.1	24.4	16.2	8.2	85	-	-
213	350	9.8	0.443	225.1	0.025	0.014	0.011	-	-	-

Table 1. Calculated values of maturation level (effective %Ro), temperature and realization of hydrocarbon potential for the probably source rocks in the present-day sedimentary sections in the Admiralteyskoe Rise of the East Barents Sea Basin. (See additional table notes.)

T	Z	T	Ro	Hi	Ht	Ho	Hg	t1	texp	t2
My	M	°C	%	Mg HC/g Corg				Million years ago		
Ludlovskaya area										
387	12750	274.5	4.670	487	487	0.	262	266	254.6	235
290	10750	244.8	4.317	619	619	0.	336	240	237.0	227
246	8750	206.4	3.431	225.1	225	0.002	161	229	213.7	217
228	5500	142.0	1.551	225.1	200	47.4	116	217	212.6	141
216	3250	92.0	0.772	225.1	67.2	46.5	20.7	143	-	-
213	2675	78.9	0.675	225.1	14.2	9.08	5.12	-	-	-
Ledovaya area										
387	17700	383.6	4.690	487	487	0.	262	345	321.1	289
290	12200	299.2	4.690	619	619	0.	336	252	241.9	233
246	9700	247.1	4.408	225.1	225	0.	161	232	228.0	222
231	6450	176	2.637	225.1	218	0.007	155	224	218.9	209
214.5	3000	95	0.829	225.1	103	71.8	31.3	173	-	-
213	2700	86.3	0.758	225.1	57.1	39.6	17.5	100	-	-
Shtockman area										
387	16000	366.8	4.690	487	487	0.	262	275	270.2	258
286	13600	331.8	4.690	619	619	0.	336	259	254.5	241
243	9650	252	4.376	225.1	225	0.	161	231	226.6	222
229	6400	181.5	2.626	225.1	217	0.005	154	223	218.6	210
219	4000	125.9	1.240	225.1	185	107	73.5	211	203	-
213	2650	90.9	0.764	225.1	61.7	42.8	18.9	78	-	-
Arctic area										
387	16500	346.3	4.690	487	487	0.	262	281	275	263
286	13500	307.1	4.690	619	619	0.	336	260	255.7	246
243	9500	233.3	4.030	225.1	225	0.	161	235	232	229
236	6340	170.7	2.303	225.1	211	0.027	149	230.7	226.2	213
231	4330	128.1	1.260	225.1	187	110	73.7	135	107.8	-
225	3400	106.4	0.901	225.1	138	98	40	110	-	-
213	3130	99.8	0.851	225.1	115	81	34	105	-	-
208	3130	99.8	0.838	627	396	386	10	104.5	-	-
144	2380	83.3	0.697	627	94.4	90.8	3.6	-	-	-

Table 2. Calculated values of maturation level (effective %Ro), temperature and realization of hydrocarbon potential for the probably source rocks in the present-day sedimentary sections in the southern part of the East Barents Sea Basin and Prirazlomnaya area of the Pechora Basin. (See additional table notes.)

Notes to Table 1 and Table 2:

t – formation age (My). z – depth (km). T – temperature in °C. Ro – vitrinite reflectance (in %; for Ordovician rocks it will be effective Ro, because vitrinite is absent in the rocks of such age). Hi – initial potential of HC generation by formation rock; Ht – total HC generation by formation rocks, Ho – oil generation and Hg – gas generation (in mg HC/g Corg). t1, t2 – times of rock enter in "oil" (Ro=0.50%) and "gas" (Ro=1.30%) "windows"; texp – time of expulsion threshold for liquid HC.

The following types of kerogene are assumed for probably source rocks:

Ordovician (t=508 My): Corg=0.4%, OM is presented by kerogene of type II with initial potential of HC generation Hi=377 mg HC/g Corg.
Middle Devonian (t=387 My): In the Pakhtusov and Admiralteyskaya areas - Corg=0.4%, OM presented by the mixture 50% kerogene of type II (HI=377) and 50% kerogene of type III (HI=160) with summary initial potential Hi=268 mg HC/g Corg; In all more southern areas including Krestovaya, - Copr=0.6%, OM presented by the mixture 70% kerogene of type II (HI=627) and 30% kerogene of type III (HI=160) with summary initial potential Hi=487 mg HC/g.

Upper Devonian (t=374 My): Corg=2%, OM presented by the mixture 50% kerogene of type I (HI=710) and 50% kerogene of type II (HI=627) with summary initial potential Hi=668.5 mg HC/g.

Upper Devonian (t=367 My): Corg=2%, OM presented by the kerogene of type II with initial potential Hi=367 mg HC/g.
Upper Devonian (t=360 My): Corg=0.3%, OM presented by the kerogene of type II with initial potential Hi=367 mg HC/g.

Carboniferous (t=359 / 290 My): In the Pakhtusov and Admiralteyskaya areas - Corg=0.4%, OM presented by the kerogene of type II with initial potential Hi=367 mg HC/g Corg; In all more southern areas including Krestovaya, - Copr=1.0%, OM presented by the mixture 30% kerogene of type I (HI=911), 50% kerogene of type II (HI=627) and 20% kerogene of type III (Hi=160) with summary initial potential Hi=619 mg HC/g.

Lower and Upper Permian (t=299/288, 271/263, 255, 248 My): Corg=0.4%, OM presented by the mixture 50% kerogene of type II (HI=367) and 50% kerogene of type III (Hi=160) with summary initial potential Hi=268 mg HC/g.

Lower, Middle and Upper Triassic (t=251, 243, 235, 231, 229, 225, 219, 214.5, 213 My): Corg=0.4%, OM presented by the mixture 30% kerogene of type II (HI=367) and 70% kerogene of type III (Hi=160) with summary initial potential Hi=225.1 mg HC/g.

Low and upper Jurassic (t=208, 144 My): Corg=3.0%, OM presented by the kerogene of type II with initial potential Hi=627 mg HC/g.